Cronfa - Swansea University Open Access Repository

_____

This is an author produced version of a paper published in:
Journal of The Royal Society Interface

_____

Cronfa URL for this paper:

http://cronfa.swan.ac.uk/Record/cronfa39546

_____

Paper:

Pant, S. (2018). Information sensitivity functions to assess parameter information gain and identifiability of dynamical systems. _Journal of The Royal Society Interface, 15_(142), 20170871

http://dx.doi.org/10.1098/rsif.2017.0871

http://www.swansea.ac.uk/library/researchsupport/ris-support/

INTERFACE

rsif.royalsocietypublishing.org

Research

Author for correspondence:
Sanjay Pant
e-mail: Sanjay.Pant@swansea.ac.uk

THE ROYAL SOCIETY
PUBLISHING

Information sensitivity functions to assess parameter information gain and identifiability of dynamical systems

Sanjay Pant

Zienkiewicz Centre for Computational Engineering, Swansea University, Swansea, UK

SP, 0000-0002-2081-308X

A new class of functions, called the 'information sensitivity functions' (ISFs), which quantify the information gain about the parameters through the measurements/observables of a dynamical system are presented. These functions can be easily computed through classical sensitivity functions alone and are based on Bayesian and information-theoretic approaches. While marginal information gain is quantified by decrease in differential entropy, correlations between arbitrary sets of parameters are assessed through mutual information. For individual parameters, these information gains are also presented as marginal posterior variances, and, to assess the effect of correlations, as conditional variances when other parameters are given. The easy to interpret ISFs can be used to (a) identify time intervals or regions in dynamical system behaviour where information about the parameters is concentrated; (b) assess the effect of measurement noise on the information gain for the parameters; (c) assess whether sufficient information in an experimental protocol (input, measurements and their frequency) is available to identify the parameters; (d) assess correlation in the posterior distribution of the parameters to identify the sets of parameters that are likely to be indistinguishable; and (e) assess identifiability problems for particular sets of parameters.

1. Introduction

Sensitivity analysis [1] has been widely used to determine how the parameters of a dynamical system influence its outputs. When one or more outputs are measured (observed), it quantifies the variation of the observations with respect to the parameters to determine which parameters are most and least influential towards the measurements. Therefore, when performing an inverse problem of estimating the parameters from the measurements, sensitivity analysis is widely used to fix the least influential parameters (as their effect on the measurements is insignificant and removing them reduces the dimensionality of the inverse problem) while focussing on estimation of the most influential parameters. Sensitivity analysis is also used to assess the question of parameter identifiability, i.e. how easy or difficult is it to identify the parameters from the measurements. This is primarily based on the idea that if the observables are highly sensitive to perturbations in certain parameters then these parameters are likely to be identifiable, and if the observables are insensitive then the parameters are likely to be unidentifiable. However, the magnitude of the sensitivities is hard to interpret, except in the trivial case when the sensitivities are identically zero. Lastly, parameter identifiability based on sensitivity analysis also assesses correlation/dependence between the parameters—through principle component analysis [2], correlation method [3], orthogonal method [4] and the eigenvalue method [5]—to identify which pairs of parameters, owing to the high correlation, are likely to be indistinguishable from each other (also see [6] and the referenced therein). Another method to assess correlations is based on the Fisher information matrix [6–8], which can be derived from asymptotic analysis of nonlinear least-squares estimators [9,10]. Ashyraliyev & Blom [11] suggested that a singular value decomposition of the Fisher information matrix can be used to identify linear combinations of parameters that can be well

identified given the observables and measurement noise. Another class of methods to assess identifiability, proposed by Raue et al. [12–14], are based on the exploiting the curvature of the likelihood function or the flatness of the profile likelihood, i.e. minimization of the likelihood with respect to all parameters but one. Li & Vu [15,16] proposed that pairwise and higher-order correlations between the parameters may be identified by assessing linear dependencies between the columns of the sensitivity matrix [16] or the matrix of first-order partial derivatives of the state equations [15]. Thomaseth and Cobeli extended the classical sensitivity functions to 'generalized sensitivity functions' (GSFs) which assess information gain about the parameters from the measurements. This method has been widely used to assess identifiability of dynamical systems [10,17–20], where regions of high information gain show a sharp increase in the GSFs while oscillations imply correlation with other parameters. There are two drawbacks of GSFs: first, that they are designed to start at 0 and end at 1, which leads to the so-called 'force-to-one' phenomenon, where even in the absence of information about the parameters the GSFs are forces to end at a value of 1; and second, oscillations in GSFs can be hard to interpret in terms of identifying which sets of parameters are correlated. Based on a pure information-theoretic approach Pant & Lombardi [21] proposed to compute information gain through a decrease in Shannon entropy, which alleviated the shortcomings of GSFs. However, since their method relies on a Monte Carlo type method the computational effort associated with the computation of information gains can be quite large. In this article, a novel method which combines the method of Pant & Lombardi [21] with the classical sensitivity functions to compute information gain about the parameters is presented. The new functions are collectively called 'information sensitivity functions' (ISFs), which assess parameter information gain through sensitivity functions alone, thereby eliminating the need for Monte Carlo runs. These functions (i) are based on Bayesian/information-theoretic methods and do not rely on asymptotic analysis; (ii) are monotonically non-decreasing and therefore do not oscillate; (iii) can assess regions of high information content for individual parameters; (iv) can assess parameter correlations between an arbitrary set of parameters; (v) can reveal potential problems in identifiability of system parameters; (vi) can assess the effect of experimental protocol on the inverse problem, for example, which outputs are measured, associated measurement noise, and measurement frequency; and (vii) are easily interpretable.

In what follows, first the theoretic developments are presented in §§2–8, followed by their application to three different dynamical systems in §9. The three examples are chosen from different areas in mathematical biosciences: (i) a Windkessel model, which is a widely used boundary condition in computational fluid dynamics simulations of haemodynamics; (ii) the Hodgkin–Huxley model for a biological neuron, which has formed the basis for a variety of ionic models describing excitable tissues; and (iii) a kinetics model for the influenza A virus.

2. The dynamical system and sensitivity equations

Consider the following dynamical system governed by a set of parametrized ordinary differential equations (ODEs):

$$\dot{\mathbf{x}} = \mathbf{f}(\mathbf{x}, \boldsymbol{\theta}, t) \quad \text{with } \mathbf{x}(t_0) = \mathbf{x}_0, \tag{2.1}$$

where t represents time, $\mathbf{x} \in \mathbb{R}^d$ is the state vector, $\boldsymbol{\theta} \in \mathbb{R}^p$ is the parameter vector, the function $\mathbf{f}: \mathbb{R}^{d+p+1} \to \mathbb{R}^d$ represents the dynamics and $\mathbf{x}_0$ represents the initial condition at time t_0. The initial conditions may depend on the parameters, and therefore

$$\mathbf{x}(t_0) = \mathbf{x}_0(\boldsymbol{\theta}). \tag{2.2}$$

The above representation subsumes the case where the initial condition may itself be seen as a parameter. The RHS of the dynamical system, equation (2.1), can be linearized at at a reference point $(\mathbf{x}_r, \boldsymbol{\theta}_r, t_r)$, to obtain

$$\dot{\mathbf{x}} = \mathbf{f}(\mathbf{x}, \boldsymbol{\theta}, t)|_r + \nabla_{\mathbf{x}}\mathbf{f}(\mathbf{x}, \boldsymbol{\theta}, t)|_r(\mathbf{x} - \mathbf{x}_r) + \nabla_{\boldsymbol{\theta}}\mathbf{f}(\mathbf{x}, \boldsymbol{\theta}, t)|_r(\boldsymbol{\theta} - \boldsymbol{\theta}_r)$$
$$+ \nabla_t\mathbf{f}(\mathbf{x}, \boldsymbol{\theta}, t)|_r(t - t_r) + \mathcal{O}(2), \tag{2.3}$$

where $(\cdot)|_r$ represents $(\cdot)$ evaluated at the reference point. Henceforth, in order to be concise, the explicit dependence of $\mathbf{f}(\mathbf{x}, \boldsymbol{\theta}, t)$ on its arguments is omitted and $\mathbf{f}$, without any arguments, is used to denote $\mathbf{f}(\mathbf{x}, \boldsymbol{\theta}, t)$. Following this notation, equation (2.3) is concisely written as

$$\dot{\mathbf{x}} = \mathbf{f}|_r + \nabla_{\mathbf{x}}\mathbf{f}|_r(\mathbf{x} - \mathbf{x}_r) + \nabla_{\boldsymbol{\theta}}\mathbf{f}|_r(\boldsymbol{\theta} - \boldsymbol{\theta}_r) + \nabla_t\mathbf{f}|_r(t - t_r)$$
$$+ \mathcal{O}(2). \tag{2.4}$$

The above linearization will be used in the next section to study the evolution of the state covariance matrix with time. Let $\mathbf{S} \in \mathbb{R}^{d \times p}$ denote the matrix of sensitivity functions for the system in equation (2.1), i.e. $\mathbf{S} = \nabla_{\boldsymbol{\theta}}\mathbf{x}$, or

$$S_{i,j} = \frac{\partial x_i}{\partial \theta_j}. \tag{2.5}$$

It is well known that $\mathbf{S}$ satisfies the following ODE system, which can be obtained by applying the chain rule of differentiation to equation (2.1):

$$\dot{\mathbf{S}} = (\nabla_{\mathbf{x}}\mathbf{f}(\mathbf{x},\boldsymbol{\theta},t))\mathbf{S} + \nabla_{\boldsymbol{\theta}}\mathbf{f}(\mathbf{x},\boldsymbol{\theta},t) \quad \text{with } \mathbf{S}(t_0) = \nabla_{\boldsymbol{\theta}}(\mathbf{x}_0(\boldsymbol{\theta})). \tag{2.6}$$

The goal is to relate the evolution of the sensitivity matrix to the evolution of the covariance of the joint vector of the state and the parameters. Let the subscript n denote all quantities at time t_n; for example, $\mathbf{x}_n$ denotes the state vector at time t_n, $\mathbf{S}_n$ the corresponding sensitivity matrix, and so on. To relate the sensitivity matrix $\mathbf{S}_{n+1}$ at time t_{n+1} with $\mathbf{S}_n$, a first-order discretization of equation (2.6) is considered

$$\frac{\mathbf{S}_{n+1} - \mathbf{S}_n}{\Delta t} = \nabla_{\mathbf{x}}\mathbf{f}|_n\mathbf{S}_n + \nabla_{\boldsymbol{\theta}}\mathbf{f}|_n \tag{2.7}$$

and, therefore, the matrix product $\mathbf{S}_{n+1}\mathbf{S}_{n+1}^{\mathsf{T}}$ can be written as

$$\mathbf{S}_{n+1}\mathbf{S}_{n+1}^{\mathsf{T}} = \mathbf{S}_n\mathbf{S}_n^{\mathsf{T}} + \mathbf{S}_n\mathbf{S}_n^{\mathsf{T}}(\nabla_{\mathbf{x}}^{\mathsf{T}}\mathbf{f}|_n)\Delta t + \mathbf{S}_n(\nabla_{\boldsymbol{\theta}}^{\mathsf{T}}\mathbf{f}|_n)\Delta t$$
$$+ (\nabla_{\mathbf{x}}\mathbf{f}|_n)\mathbf{S}_n\mathbf{S}_n^{\mathsf{T}}\Delta t + (\nabla_{\mathbf{x}}\mathbf{f}|_n)\mathbf{S}_n\mathbf{S}_n^{\mathsf{T}}(\nabla_{\mathbf{x}}^{\mathsf{T}}\mathbf{f}|_n)\Delta t^2$$
$$+ (\nabla_{\mathbf{x}}\mathbf{f}|_n)\mathbf{S}_n(\nabla_{\boldsymbol{\theta}}^{\mathsf{T}}\mathbf{f}|_n)\Delta t^2 + (\nabla_{\boldsymbol{\theta}}\mathbf{f}|_n)\mathbf{S}_n^{\mathsf{T}}\Delta t$$
$$+ (\nabla_{\boldsymbol{\theta}}\mathbf{f}|_n)\mathbf{S}_n^{\mathsf{T}}(\nabla_{\mathbf{x}}^{\mathsf{T}}\mathbf{f}|_n)\Delta t^2 + (\nabla_{\boldsymbol{\theta}}\mathbf{f}|_n)(\nabla_{\boldsymbol{\theta}}^{\mathsf{T}}\mathbf{f}|_n)\Delta t^2. \tag{2.8}$$

Next, it is hypothesized that under certain conditions $\mathbf{S}_{n+1}\mathbf{S}_{n+1}^{\mathsf{T}}$ can be seen as the covariance matrix of the state vector at time t_{n+1}. These developments are presented in the next two sections.

3. Forward propagation of uncertainty

As the objective is to study the relationship between the parameters and the state vector, a joint vector of all the state vectors until the current time t_n and the parameter vector is considered. Assume that at time t_n, this joint

2

vector $[\mathbf{x}_n^\mathsf{T}, \mathbf{x}_{n-1}^\mathsf{T}, \ldots, \mathbf{x}_0^\mathsf{T}, \boldsymbol{\theta}^\mathsf{T}]^\mathsf{T}$ is distributed according to a multivariate Normal distribution as follows:

$$
\begin{bmatrix} \mathbf{x}_n \\ \mathbf{x}_{n-1} \\ \vdots \\ \mathbf{x}_0 \\ \boldsymbol{\theta} \end{bmatrix} \sim \mathcal{N}\left(\boldsymbol{\mu}_n = \begin{bmatrix} \boldsymbol{\mu}_{\mathbf{x}_n} \\ \boldsymbol{\mu}_{\mathbf{x}_{n-1}} \\ \vdots \\ \boldsymbol{\mu}_{\mathbf{x}_0} \\ \boldsymbol{\mu}_{\boldsymbol{\theta}} \end{bmatrix}, \boldsymbol{\Sigma}_n = \begin{bmatrix} \boldsymbol{\Sigma}_{n,n} & \boldsymbol{\Sigma}_{n,n-1} & \cdots & \boldsymbol{\Sigma}_{n,0} & \boldsymbol{\Lambda}_{n,\boldsymbol{\theta}} \\ \boldsymbol{\Sigma}_{n-1,n} & \boldsymbol{\Sigma}_{n-1,n-1} & \cdots & \boldsymbol{\Sigma}_{n-1,0} & \boldsymbol{\Lambda}_{n-1,\boldsymbol{\theta}} \\ \vdots & \vdots & \ddots & \vdots & \vdots \\ \boldsymbol{\Sigma}_{0,n} & \boldsymbol{\Sigma}_{0,n-1} & \cdots & \boldsymbol{\Sigma}_{0,0} & \boldsymbol{\Lambda}_{0,\boldsymbol{\theta}} \\ \boldsymbol{\Lambda}_{\boldsymbol{\theta},n} & \boldsymbol{\Lambda}_{\boldsymbol{\theta},n-1} & \cdots & \boldsymbol{\Lambda}_{\boldsymbol{\theta},0} & \boldsymbol{\Sigma}_{\boldsymbol{\theta},\boldsymbol{\theta}} \end{bmatrix} \right).
$$

(3.1)

To obtain the joint distribution of $[\mathbf{x}_{n+1}^\mathsf{T}, \mathbf{x}_n^\mathsf{T}, \ldots, \mathbf{x}_0^\mathsf{T}, \boldsymbol{\theta}^\mathsf{T}]^\mathsf{T}$ (all the state vectors until time t_{n+1} and the parameter vector), the linearized dynamical system, equation (2.4), is used. Considering the reference point $(\mathbf{x}_r, \boldsymbol{\theta}_r, t_r)$ in equation (2.4) to be $(\boldsymbol{\mu}_{\mathbf{x}_n}, \boldsymbol{\mu}_{\boldsymbol{\theta}}, t_n)$, i.e. considering the linearization around the mean values of the parameter vector and the state at time t_n, one obtains

$$\dot{\mathbf{x}} = \mathbf{f}|_n + \nabla_{\mathbf{x}}\mathbf{f}|_n(\mathbf{x} - \boldsymbol{\mu}_{\mathbf{x}_n}) + \nabla_{\boldsymbol{\theta}}\mathbf{f}|_n(\boldsymbol{\theta} - \boldsymbol{\mu}_{\boldsymbol{\theta}}) + \nabla_t\mathbf{f}|_n(t - t_n) + \mathcal{O}(2).$$

(3.2)

Ignoring the higher-order terms, and employing a forward Euler discretization, one obtains

$$\mathbf{x}_{n+1} \approx \mathbf{x}_n + \mathbf{f}|_n\Delta t + \nabla_{\mathbf{x}}\mathbf{f}|_n(\mathbf{x}_n - \boldsymbol{\mu}_{\mathbf{x}_n})\Delta t + \nabla_{\boldsymbol{\theta}}\mathbf{f}|_n(\boldsymbol{\theta} - \boldsymbol{\mu}_{\boldsymbol{\theta}})\Delta t.$$

(3.3)

Remark 3.1. $\mathbf{x}_{n+1}$ is completely determined by $\mathbf{x}_n$ and $\boldsymbol{\theta}$, i.e. given $\mathbf{x}_n$ and $\boldsymbol{\theta}$ nothing more can be learned about $\mathbf{x}_{n+1}$. Hence, the forward propagation forms a Markov chain.

Remark 3.2. $\mathbf{f}|_n, \nabla_{\mathbf{x}}\mathbf{f}|_n, \nabla_{\boldsymbol{\theta}}\mathbf{f}|_n$ are evaluated at $(\boldsymbol{\mu}_{\mathbf{x}_n}, \boldsymbol{\mu}_{\boldsymbol{\theta}}, t_n)$.

Remark 3.3. In equation (3.1), $\boldsymbol{\Sigma}_{\alpha,\beta} = \boldsymbol{\Sigma}_{\beta,\alpha}^\mathsf{T}$ and $\boldsymbol{\Lambda}_{\alpha,\beta} = \boldsymbol{\Lambda}_{\beta,\alpha}^\mathsf{T}$.

The joint vector $[\mathbf{x}_{n+1}^\mathsf{T}, \mathbf{x}_n^\mathsf{T}, \ldots, \mathbf{x}_0^\mathsf{T}, \boldsymbol{\theta}^\mathsf{T}]^\mathsf{T}$ can be written from equations (3.1) and (3.3) as

$$
\underbrace{\begin{bmatrix} \mathbf{x}_{n+1} \\ \mathbf{x}_n \\ \mathbf{x}_{n-1} \\ \vdots \\ \mathbf{x}_0 \\ \boldsymbol{\theta} \end{bmatrix}}_{} \approx \underbrace{\begin{bmatrix} \mathbf{I}_d + \nabla_{\mathbf{x}}\mathbf{f}|_n\Delta t & \mathbf{O}_{d,d} & \mathbf{O}_{d,d} & \cdots & \mathbf{O}_{d,d} & \nabla_{\boldsymbol{\theta}}\mathbf{f}|_n\Delta t \\ \mathbf{I}_d & \mathbf{O}_{d,d} & \mathbf{O}_{d,d} & \cdots & \mathbf{O}_{d,d} & \mathbf{O}_{d,p} \\ \mathbf{O}_{d,d} & \mathbf{I}_d & \mathbf{O}_{d,d} & \cdots & \mathbf{O}_{d,d} & \mathbf{O}_{d,p} \\ \vdots & \vdots & \vdots & \ddots & \vdots & \vdots \\ \mathbf{O}_{d,d} & \mathbf{O}_{d,d} & \mathbf{O}_{d,d} & \cdots & \mathbf{I}_d & \mathbf{O}_{d,p} \\ \mathbf{O}_{p,d} & \mathbf{O}_{p,d} & \mathbf{O}_{p,d} & \cdots & \mathbf{O}_{p,d} & \mathbf{I}_p \end{bmatrix}}_{\mathbf{F}_n} \begin{bmatrix} \mathbf{x}_n \\ \mathbf{x}_{n-1} \\ \vdots \\ \mathbf{x}_0 \\ \boldsymbol{\theta} \end{bmatrix} + \underbrace{\begin{bmatrix} \mathbf{C}_n \\ \mathbf{O}_{d,1} \\ \mathbf{O}_{d,1} \\ \vdots \\ \mathbf{O}_{d,1} \\ \mathbf{O}_{p,1} \end{bmatrix}}_{\mathbf{g}_n},
$$

(3.4)

where $\mathbf{I}_q$ represents an identity matrix of size q, $\mathbf{O}_{q,r}$ represents a zero matrix of size $q \times r$, and

$$\mathbf{C}_n = \mathbf{f}|_n\Delta t - \nabla_{\mathbf{x}}\mathbf{f}|_n\boldsymbol{\mu}_{\mathbf{x}_n}\Delta t - \nabla_{\boldsymbol{\theta}}\mathbf{f}|_n\boldsymbol{\mu}_{\boldsymbol{\theta}}\Delta t \quad (3.5)$$

is a term that does not depend on $\mathbf{x}_n$ and $\boldsymbol{\theta}$. The distribution of $[\mathbf{x}_{n+1}^\mathsf{T}, \mathbf{x}_n^\mathsf{T}, \ldots, \mathbf{x}_0^\mathsf{T}, \boldsymbol{\theta}^\mathsf{T}]^\mathsf{T}$ can be written from equation (3.4) as

$$[\mathbf{x}_{n+1}^\mathsf{T}, \mathbf{x}_n^\mathsf{T}, \ldots, \mathbf{x}_0^\mathsf{T}, \boldsymbol{\theta}]^\mathsf{T} \sim \mathcal{N}(\boldsymbol{\mu}_{n+1} = \mathbf{F}_n\boldsymbol{\mu}_n + \mathbf{g}_n, \boldsymbol{\Sigma}_{n+1}$$
$$= \mathbf{F}_n\boldsymbol{\Sigma}_n\mathbf{F}_n^\mathsf{T}) \quad (3.6)$$

and the covariance $\boldsymbol{\Sigma}_{n+1}$ can be expanded as

$$
\boldsymbol{\Sigma}_{n+1} = \begin{bmatrix} \boldsymbol{\Sigma}_{n+1,n+1} & \boldsymbol{\Sigma}_{n+1,n} & \boldsymbol{\Sigma}_{n+1,n-1} & \cdots & \boldsymbol{\Sigma}_{n+1,0} & \boldsymbol{\Lambda}_{n+1,\boldsymbol{\theta}} \\ \boldsymbol{\Sigma}_{n+1,n}^\mathsf{T} & \boldsymbol{\Sigma}_{n,n} & \boldsymbol{\Sigma}_{n,n-1} & \cdots & \boldsymbol{\Sigma}_{n,0} & \boldsymbol{\Lambda}_{n,\boldsymbol{\theta}} \\ \boldsymbol{\Sigma}_{n+1,n-1}^\mathsf{T} & \boldsymbol{\Sigma}_{n,n-1}^\mathsf{T} & \boldsymbol{\Sigma}_{n-1,n-1} & \cdots & \boldsymbol{\Sigma}_{n-1,0} & \boldsymbol{\Lambda}_{n-1,\boldsymbol{\theta}} \\ \vdots & \vdots & \vdots & \ddots & \vdots & \vdots \\ \boldsymbol{\Sigma}_{n,0}^\mathsf{T} & \boldsymbol{\Sigma}_{n,0}^\mathsf{T} & \boldsymbol{\Sigma}_{n-1,0}^\mathsf{T} & \cdots & \boldsymbol{\Sigma}_{0,0} & \boldsymbol{\Lambda}_{0,\boldsymbol{\theta}} \\ \boldsymbol{\Lambda}_{n,\boldsymbol{\theta}}^\mathsf{T} & \boldsymbol{\Lambda}_{n,\boldsymbol{\theta}}^\mathsf{T} & \boldsymbol{\Lambda}_{n-1,\boldsymbol{\theta}}^\mathsf{T} & \cdots & \boldsymbol{\Lambda}_{0,\boldsymbol{\theta}}^\mathsf{T} & \boldsymbol{\Sigma}_{\boldsymbol{\theta},\boldsymbol{\theta}} \end{bmatrix},
$$

(3.7)

where

$$\boldsymbol{\Sigma}_{n+1,n+1} = ((\mathbf{I}_d + \nabla_{\mathbf{x}}\mathbf{f}|_n\Delta t)\boldsymbol{\Sigma}_{n,n} + \nabla_{\boldsymbol{\theta}}^\mathsf{T}\mathbf{f}|_n\boldsymbol{\Lambda}_{n,\boldsymbol{\theta}}^\mathsf{T}\Delta t)(\mathbf{I}_d + \nabla_{\mathbf{x}}^\mathsf{T}\mathbf{f}|_n\Delta t)$$
$$+ (\nabla_{\boldsymbol{\theta}}\mathbf{f}|_n\boldsymbol{\Sigma}_{\boldsymbol{\theta},\boldsymbol{\theta}}\Delta t + (\mathbf{I}_d + \nabla_{\mathbf{x}}^\mathsf{T}\mathbf{f}|_n\Delta t)\boldsymbol{\Lambda}_{n,\boldsymbol{\theta}})\nabla_{\boldsymbol{\theta}}^\mathsf{T}\mathbf{f}|_n\Delta t, \quad (3.8)$$

$$\boldsymbol{\Lambda}_{n+1,\boldsymbol{\theta}} = (\mathbf{I}_d + \nabla_{\mathbf{x}}\mathbf{f}|_n\Delta t)\boldsymbol{\Lambda}_{n,\boldsymbol{\theta}} + \nabla_{\boldsymbol{\theta}}\mathbf{f}|_n\boldsymbol{\Sigma}_{\boldsymbol{\theta},\boldsymbol{\theta}}\Delta t \quad (3.9)$$

and

$$\boldsymbol{\Sigma}_{n+1,j} = (\mathbf{I}_d + \nabla_{\mathbf{x}}\mathbf{f}|_n\Delta t)\boldsymbol{\Sigma}_{n,j} + \nabla_{\boldsymbol{\theta}}\mathbf{f}|_n\boldsymbol{\Lambda}_{j,\boldsymbol{\theta}}^\mathsf{T}\Delta t$$
$$\text{for } 0 \leq j \leq n. \quad (3.10)$$

If the above evolution of the covariance matrix can be related to the evolution of the sensitivity matrix, as presented in §2 and equation (2.8), then the dependencies between the state vector and the parameters can be studied. This concept is developed in the next section.

4. Relationship between sensitivity and forward propagation of uncertainty

In this section, the relationship between the evolution of the sensitivity matrix and the evolution of the covariance matrix of the joint distribution between all the state vectors until time t_n and the parameters is developed. Equation (3.8) can be expanded as follows:

$$\boldsymbol{\Sigma}_{n+1,n+1} = \boldsymbol{\Sigma}_{n,n} + \nabla_{\mathbf{x}}\mathbf{f}|_n\boldsymbol{\Sigma}_{n,n}\Delta t + \nabla_{\boldsymbol{\theta}}^\mathsf{T}\mathbf{f}|_n\boldsymbol{\Lambda}_{n,\boldsymbol{\theta}}^\mathsf{T}\Delta t$$
$$+ \boldsymbol{\Sigma}_{n,n}\nabla_{\mathbf{x}}^\mathsf{T}\mathbf{f}|_n\Delta t + \nabla_{\mathbf{x}}\mathbf{f}|_n\boldsymbol{\Sigma}_{n,n}\nabla_{\mathbf{x}}^\mathsf{T}\mathbf{f}|_n\Delta t^2$$
$$+ \nabla_{\boldsymbol{\theta}}^\mathsf{T}\mathbf{f}|_n\boldsymbol{\Lambda}_{n,\boldsymbol{\theta}}^\mathsf{T}\nabla_{\mathbf{x}}^\mathsf{T}\mathbf{f}|_n\Delta t^2 + \nabla_{\boldsymbol{\theta}}\mathbf{f}|_n\boldsymbol{\Sigma}_{\boldsymbol{\theta},\boldsymbol{\theta}}\nabla_{\boldsymbol{\theta}}^\mathsf{T}\mathbf{f}|_n\Delta t^2$$
$$+ \boldsymbol{\Lambda}_{n,\boldsymbol{\theta}}\nabla_{\boldsymbol{\theta}}^\mathsf{T}\mathbf{f}|_n\Delta t + \nabla_{\mathbf{x}}^\mathsf{T}\mathbf{f}|_n\boldsymbol{\Lambda}_{n,\boldsymbol{\theta}}\nabla_{\boldsymbol{\theta}}^\mathsf{T}\mathbf{f}|_n\Delta t^2. \quad (4.1)$$

4

Assume the following:

$$\boldsymbol{\Sigma}_{n,n} = \mathbf{S}_n\mathbf{S}_n^\mathsf{T}, \tag{4.2}$$

$$\boldsymbol{\Lambda}_{n,\boldsymbol{\theta}} = \mathbf{S}_n \tag{4.3}$$

and

$$\boldsymbol{\Sigma}_{\boldsymbol{\theta},\boldsymbol{\theta}} = \mathbf{I}_p. \tag{4.4}$$

Under the above assumptions, it can be deduced from equations (4.1) and (2.8) that

$$\boldsymbol{\Sigma}_{n+1,n+1} = \mathbf{S}_{n+1}\mathbf{S}_{n+1}^\mathsf{T}. \tag{4.5}$$

Furthermore, equation (3.9) reads

$$\boldsymbol{\Lambda}_{n+1,\boldsymbol{\theta}} = (\mathbf{I}_d + \nabla_\mathbf{x}\mathbf{f}|_n\Delta t)\mathbf{S}_n + \nabla_{\boldsymbol{\theta}}\mathbf{f}|_n\Delta t,$$

which, as evident from equation (2.7), is the standard forward propagation of the sensitivity matrix. Hence

$$\boldsymbol{\Lambda}_{n+1,\boldsymbol{\theta}} = \mathbf{S}_{n+1}. \tag{4.6}$$

Finally, the term $\boldsymbol{\Sigma}_{n+1,n}$ from equation (3.10) can be written as

$$\boldsymbol{\Sigma}_{n+1,n} = \mathbf{S}_{n+1}\mathbf{S}_n^\mathsf{T}. \tag{4.7}$$

From equations (4.5), (4.6) and (4.7), it can be concluded that if the initial *prior* uncertainty in $[\mathbf{x}_0^\mathsf{T}, \boldsymbol{\theta}]^\mathsf{T}$ is assumed to be Gaussian with covariance

$$\mathbf{Cov}\left(\begin{bmatrix}\mathbf{x}_0\\\boldsymbol{\theta}\end{bmatrix}\right) = \boldsymbol{\Sigma}_0 = \begin{bmatrix}\mathbf{S}_0\mathbf{S}_0^\mathsf{T} & \mathbf{S}_0\\ \mathbf{S}_0^\mathsf{T} & \mathbf{I}_p\end{bmatrix}, \tag{4.8}$$

then the joint vector of $\boldsymbol{\theta}$, the parameters, and $[\mathbf{x}_n^\mathsf{T}, \mathbf{x}_{n-1}^\mathsf{T}, \ldots, \mathbf{x}_0^\mathsf{T}]^\mathsf{T}$, the state-vector corresponding to time instants $[t_0, t_1, \ldots, t_n]$, can be approximated, by considering only the first-order terms after linearization, to be a Gaussian distribution with the following covariance:

$$\mathbf{Cov}\begin{pmatrix}\mathbf{x}_n\\\mathbf{x}_{n-1}\\\vdots\\\mathbf{x}_0\\\boldsymbol{\theta}\end{pmatrix} = \boldsymbol{\Sigma}_n = \left[\begin{array}{ccccc|c} \mathbf{S}_n\mathbf{S}_n^\mathsf{T} & \mathbf{S}_n\mathbf{S}_{n-1}^\mathsf{T} & \mathbf{S}_n\mathbf{S}_{n-2}^\mathsf{T} & \cdots & \mathbf{S}_n\mathbf{S}_0^\mathsf{T} & \mathbf{S}_n \\ \mathbf{S}_{n-1}\mathbf{S}_n^\mathsf{T} & \mathbf{S}_{n-1}\mathbf{S}_{n-1}^\mathsf{T} & \mathbf{S}_{n-1}\mathbf{S}_{n-2}^\mathsf{T} & \cdots & \mathbf{S}_{n-1}\mathbf{S}_0^\mathsf{T} & \mathbf{S}_{n-1} \\ \mathbf{S}_{n-2}\mathbf{S}_n^\mathsf{T} & \mathbf{S}_{n-2}\mathbf{S}_{n-1}^\mathsf{T} & \mathbf{S}_{n-2}\mathbf{S}_{n-2}^\mathsf{T} & \cdots & \mathbf{S}_{n-2}\mathbf{S}_0^\mathsf{T} & \mathbf{S}_{n-2} \\ \vdots & \vdots & \vdots & \ddots & \vdots & \vdots \\ \mathbf{S}_0\mathbf{S}_n^\mathsf{T} & \mathbf{S}_0\mathbf{S}_{n-1}^\mathsf{T} & \mathbf{S}_0\mathbf{S}_{n-2}^\mathsf{T} & \cdots & \mathbf{S}_0\mathbf{S}_0^\mathsf{T} & \mathbf{S}_0 \\ \hline \mathbf{S}_n^\mathsf{T} & \mathbf{S}_{n-1}^\mathsf{T} & \mathbf{S}_{n-2}^\mathsf{T} & \cdots & \mathbf{S}_0^\mathsf{T} & \mathbf{I}_p \end{array}\right]. \tag{4.9}$$

Remark 4.1. Note that *a prior* mean for the vector $[\mathbf{x}_0^\mathsf{T}, \boldsymbol{\theta}^\mathsf{T}]^\mathsf{T}$ is assumed to be

$$\mathbf{Mean}\left(\begin{bmatrix}\mathbf{x}_0\\\boldsymbol{\theta}\end{bmatrix}\right) = \boldsymbol{\mu}_0 = \begin{bmatrix}\boldsymbol{\mu}_{\mathbf{x}_0}\\\boldsymbol{\mu}_{\boldsymbol{\theta}}\end{bmatrix} \tag{4.10}$$

based on which the mean vector of the state will propagate according to equation (3.3), essentially according to the forward Euler method. While this propagated mean does not directly influence the *posterior* uncertainty of the parameters, which depends only on the covariance matrix, it is important to note that the sensitivity terms in the covariance matrix of equation (4.9) are evaluated at the propagated means. The propagated mean of the joint vector $[\mathbf{x}_n^\mathsf{T}, \mathbf{x}_{n-1}^\mathsf{T}, \ldots, \mathbf{x}_0^\mathsf{T}, \boldsymbol{\theta}^\mathsf{T}]^\mathsf{T}$ is referred throughout this manuscript as $\boldsymbol{\mu}_n = [\boldsymbol{\mu}_{\mathbf{x}_n}^\mathsf{T}, \boldsymbol{\mu}_{\mathbf{x}_{n-1}}^\mathsf{T}, \ldots, \boldsymbol{\mu}_{\mathbf{x}_0}^\mathsf{T}, \boldsymbol{\mu}_{\boldsymbol{\theta}}^\mathsf{T}]^\mathsf{T}$.

Remark 4.2. The required conditions presented in equations (4.2), (4.3) and (4.4), can also be derived without temporal discretization of the sensitivity and linearized forward model. This is presented in appendix A, which presents a differential equation describing the evolution of the joint covariance matrix, leading to the conditions derived above without temporal discretization. Even though the method presented in appendix A may be considered more general, the author first conceived the idea using the arguments shown above, and hence these ideas are presented in the main text.

5. Measurements (observations)

Having established how the covariance of the state and the parameters evolves in relation to the sensitivity matrix, the next task is to extend this framework to include the measurements. Eventually, one wants to obtain an expression for the joint distribution of the measurements and the parameters, so that conditioning this joint distribution on the measurements (implying that measurements are known) will yield information about how much can be learned about the parameters.

Consider a linear observation operator where $\mathbf{y}_n \in \mathbb{R}^m$ is measured at time t_n according to

$$\mathbf{y}_n = \mathbf{H}_n\mathbf{x}_n + \boldsymbol{\epsilon}_n, \tag{5.1}$$

where $\mathbf{H}_n \in \mathbb{R}^{m\times d}$ is the observation operator at time t_n and $\boldsymbol{\epsilon}_n$ is the measurement noise. Let $\boldsymbol{\epsilon}_n$ be independently (across all measurement times) distributed as

$$\boldsymbol{\epsilon}_n \sim \mathcal{N}(\mathbf{O}_m, \mathbf{Y}_n), \tag{5.2}$$

where $\mathbf{O}_m$ is a zero vector and $\mathbf{Y}_n$ is the covariance structure of the noise. From equations (4.9) and (5.1), it is easy to see that $[\mathbf{y}_n^\mathsf{T}, \mathbf{y}_{n-1}^\mathsf{T}, \ldots, \mathbf{y}_0^\mathsf{T}, \boldsymbol{\theta}]^\mathsf{T}$ follows a Gaussian distribution with the following mean and covariance:

$$\mathbf{Mean}\left(\begin{bmatrix}\mathbf{y}_n\\\mathbf{y}_{n-1}\\\vdots\\\mathbf{y}_0\\\boldsymbol{\theta}\end{bmatrix}\right) = \boldsymbol{\alpha}_n = \begin{bmatrix}\mathbf{H}_n\boldsymbol{\mu}_{\mathbf{x}_n}\\\mathbf{H}_{n-1}\boldsymbol{\mu}_{\mathbf{x}_{n-1}}\\\vdots\\\mathbf{H}_0\boldsymbol{\mu}_{\mathbf{x}_0}\\\boldsymbol{\mu}_{\boldsymbol{\theta}}\end{bmatrix}; \quad \mathbf{Cov}\left(\begin{bmatrix}\mathbf{y}_n\\\mathbf{y}_{n-1}\\\vdots\\\mathbf{y}_0\\\boldsymbol{\theta}\end{bmatrix}\right) = \begin{bmatrix}\mathbf{A}_n & \mathbf{B}_n\\\mathbf{B}_n^\mathsf{T} & \mathbf{I}_p\end{bmatrix}, \tag{5.3}$$

where

$$\mathbf{A}_n = \begin{bmatrix} \mathbf{H}_n\mathbf{S}_n\mathbf{S}_n^\mathsf{T}\mathbf{H}_n^\mathsf{T} + \boldsymbol{Y}_n & \mathbf{H}_n\mathbf{S}_n\,\mathbf{S}_{n-1}^\mathsf{T}\,\mathbf{H}_{n-1}^\mathsf{T} & \cdots & \mathbf{H}_n\mathbf{S}_n\mathbf{S}_0^\mathsf{T}\mathbf{H}_0^\mathsf{T} \\ \mathbf{H}_{n-1}\mathbf{S}_{n-1}\mathbf{S}_n^\mathsf{T}\mathbf{H}_n^\mathsf{T} & \mathbf{H}_{n-1}\mathbf{S}_{n-1}\mathbf{S}_{n-1}^\mathsf{T}\mathbf{H}_{n-1}^\mathsf{T} + \boldsymbol{Y}_{n-1} & \cdots & \mathbf{H}_{n-1}\mathbf{S}_{n-1}\mathbf{S}_0^\mathsf{T}\mathbf{H}_0^\mathsf{T} \\ \vdots & \vdots & \ddots & \vdots \\ \mathbf{H}_0\mathbf{S}_0\mathbf{S}_n^\mathsf{T}\mathbf{H}_n^\mathsf{T} & \mathbf{H}_0\mathbf{S}_0\,\mathbf{S}_{n-1}^\mathsf{T}\,\mathbf{H}_{n-1}^\mathsf{T} & \cdots & \mathbf{H}_0\mathbf{S}_0\mathbf{S}_0^\mathsf{T}\mathbf{H}_0^\mathsf{T} + \boldsymbol{Y}_0 \end{bmatrix} \tag{5.4}$$

and

$$\mathbf{B}_n^\mathsf{T} = [\mathbf{S}_n^\mathsf{T}\mathbf{H}_n^\mathsf{T} \quad \mathbf{S}_{n-1}^\mathsf{T}\mathbf{H}_{n-1}^\mathsf{T} \quad \cdots \quad \mathbf{S}_0^\mathsf{T}\mathbf{H}_0^\mathsf{T}]. \tag{5.5}$$

Remark 5.1. A nonlinear observation operator $\mathcal{H}$ in equation (5.1), as opposed to the linear operator $\mathbf{H}$, does not present any technical challenges to the formulation as it can be linearized at the current mean values. Following this, in equations (5.4) and (5.5), $\mathbf{H}$ would need to be replaced by the tangent operator $\nabla\mathcal{H}|_n$.

6. Conditional distribution of the parameters

The quantity of interest is the conditional distribution of parameters; i.e. how the beliefs about the parameters have changed from the *prior* beliefs to the *posterior* beliefs (the conditional distribution) by the measurements. More than the mean of the conditional distribution, the covariance is of interest. This is due to two reasons: (i) owing to the Gaussian approximations, the covariance entirely reflects the amount of uncertainty in the parameters; and (ii) while the mean of the conditional distribution depends on the measurements, the covariance does not. The latter is significant because a priori, the measurement values are not known. Consequently, the average (over all possible measurements) uncertainty in the parameters too is independent of the measurements, and hence can be studied *a priori*.

From equation (5.3), since the joint distribution of the parameter vector and the observables is Gaussian, the conditional distribution of the parameter vector given the measurements is also Gaussian and can be written as

$$p(\boldsymbol{\theta}\,|\,[\mathbf{y}_n^\mathsf{T}, \mathbf{y}_{n-1}^\mathsf{T}, \ldots, \mathbf{y}_0^\mathsf{T}]^\mathsf{T}) = \mathcal{N}(\boldsymbol{\beta}_n, \mathcal{C}_n), \tag{6.1}$$

with

$$\begin{aligned}\boldsymbol{\beta}_n = \boldsymbol{\mu}_{\boldsymbol{\theta}} &+ \mathbf{B}_n^\mathsf{T}\mathbf{A}_n^{-1}([\mathbf{y}_n^{\mathrm{o}\mathsf{T}}, \mathbf{y}_{n-1}^{\mathrm{o}\mathsf{T}}, \ldots, \mathbf{y}_0^{\mathrm{o}\mathsf{T}}]^\mathsf{T} \\ &- [(\mathbf{H}_n\boldsymbol{\mu}_{\mathbf{x}_n})^\mathsf{T}, (\mathbf{H}_{n-1}\boldsymbol{\mu}_{\mathbf{x}_{n-1}})^\mathsf{T}, \ldots, (\mathbf{H}_0\boldsymbol{\mu}_{\mathbf{x}_0})^\mathsf{T}]^\mathsf{T})\end{aligned} \tag{6.2}$$

and

$$\mathcal{C}_n = \mathbf{I}_\mathrm{P} - \mathbf{B}_n^\mathsf{T}\mathbf{A}_n^{-1}\mathbf{B}_n, \tag{6.3}$$

where $\mathbf{y}_i^{\mathrm{o}}$ denotes the measurement value (the realization of the random variable $\mathbf{y}_n$ observed) at t_i. Note that the conditional covariance $\mathcal{C}_n$ is independent of these measurement values $\mathbf{y}_i^{\mathrm{o}}$. Furthermore, since the uncertainty in a Gaussian random variable, quantified by the differential entropy, depends only on the covariance matrix, the posterior distribution uncertainty does not depend on the measurements.

7. Conditional covariance when $n \to \infty$ and when n is finite

For the asymptotic case when $n \to \infty$, it can be shown that (for proof see appendix B)

$$\lim_{n\to\infty} \mathcal{C}_n = \mathcal{M}^{-1}, \tag{7.1}$$

where $\mathcal{M}$ is the Fisher information matrix defined as

$$\mathcal{M} = \sum_{i=0}^{n}[(\nabla_{\boldsymbol{\theta}}^\mathsf{T}\mathbf{x}\,|_i)\,\boldsymbol{Y}_i^{-1}(\nabla_{\boldsymbol{\theta}}\mathbf{x}\,|_i)]. \tag{7.2}$$

Furthermore, for finite n, the conditional covariance can be written as (for proof see appendix C)

$$\mathcal{C}_n = \left(\mathbf{I}_p + \sum_{i=0}^{n}(\mathbf{S}_i^\mathsf{T}\mathbf{H}_i^\mathsf{T}\,\boldsymbol{Y}_i^{-1}\mathbf{H}_i\mathbf{S}_i)\right)^{-1}. \tag{7.3}$$

Remark 7.1. Equations (7.1) and (7.3) relate to the classical and Bayesian Cramer Rao bounds [22,23], respectively, in estimation theory.

8. Information gain

In this section, the gain in information about the parameters by the measurements is considered. For details of such an information-theoretic approach the reader is referred to [21]. The gain in information about the parameter vector $\boldsymbol{\theta}$ by the measurements of $\mathbf{z}_n = [\mathbf{y}_n^\mathsf{T}, \mathbf{y}_{n-1}^\mathsf{T}, \ldots, \mathbf{y}_0^\mathsf{T}]^\mathsf{T}$ is given by the mutual information between $\mathbf{z}_n$ and $\boldsymbol{\theta}$, which is equal to the difference between the differential entropies of the prior distribution $p(\boldsymbol{\theta})$ and the conditional distribution $p(\boldsymbol{\theta}|\mathbf{z}_n)$. From equations (4.8), (6.1) and (6.3), this gain in information can be written as

$$\mathcal{I}_n = \frac{1}{2}\ln[\det(\mathbf{I}_p)] - \frac{1}{2}\ln[\det(\mathcal{C}_n)] = -\frac{1}{2}\ln[\det(\mathcal{C}_n)], \tag{8.1}$$

where $\det(\cdot)$ denotes the determinant. The above can be expanded through equation (7.3) as

$$\mathcal{I}_n = \frac{1}{2}\ln\left[\det\left(\mathbf{I}_p + \sum_{i=0}^{n}(\mathbf{S}_i^\mathsf{T}\mathbf{H}_i^\mathsf{T}\,\boldsymbol{Y}_i^{-1}\mathbf{H}_i\mathbf{S}_i)\right)\right]. \tag{8.2}$$

Note that the above represents the information gain for the joint vector of all the parameters. Commonly, one is interested in individual parameters, for which the information gain is now presented. Let $\boldsymbol{\theta}^{\{\mathcal{S}\}}$ denote the vector of a subset of parameters indexed by the elements of set $\mathcal{S}$ and $\boldsymbol{\theta}^{\{\bar{\mathcal{S}}\}}$ denote the vector of the remaining parameters, the complement of set $\mathcal{S}$. Hence, $\boldsymbol{\theta}^{\{i\}}$ denotes the ith parameter, $\boldsymbol{\theta}^{\{i,j\}}$ denotes the vector formed by taking the ith and jth parameters, and so on. The conditional covariance

matrix $\mathcal{C}_n$ can be decomposed into the components of $\boldsymbol{\theta}^{\{S\}}$ and $\boldsymbol{\theta}^{\{S^c\}}$ as

$$\mathcal{C}_n = \left(\begin{bmatrix} \mathbf{I}_s & \mathbf{O} \\ \mathbf{O} & \mathbf{I}_{p-s} \end{bmatrix} + \sum_{i=0}^{n} \begin{bmatrix} (\mathbf{S}_i^{\{S\}^{\mathsf{T}}} \mathbf{H}_i^{\mathsf{T}} \boldsymbol{\varUpsilon}_i^{-1} \mathbf{H}_i \mathbf{S}_i^{\{S\}}) & (\mathbf{S}_i^{\{S\}^{\mathsf{T}}} \mathbf{H}_i^{\mathsf{T}} \boldsymbol{\varUpsilon}_i^{-1} \mathbf{H}_i \mathbf{S}_i^{\{S^c\}}) \\ (\mathbf{S}_i^{\{S^c\}^{\mathsf{T}}} \mathbf{H}_i^{\mathsf{T}} \boldsymbol{\varUpsilon}_i^{-1} \mathbf{H}_i \mathbf{S}_i^{\{S\}}) & (\mathbf{S}_i^{\{S^c\}^{\mathsf{T}}} \mathbf{H}_i^{\mathsf{T}} \boldsymbol{\varUpsilon}_i^{-1} \mathbf{H}_i \mathbf{S}_i^{\{S^c\}}) \end{bmatrix} \right)^{-1} \tag{8.3}$$

and

$$\mathcal{C}_n = \left(\begin{bmatrix} \mathbf{I}_s & \mathbf{O} \\ \mathbf{O} & \mathbf{I}_{p-s} \end{bmatrix} + \begin{bmatrix} \overbrace{\sum_{i=0}^{n} (\mathbf{S}_i^{\{S\}^{\mathsf{T}}} \mathbf{H}_i^{\mathsf{T}} \boldsymbol{\varUpsilon}_i^{-1} \mathbf{H}_i \mathbf{S}_i^{\{S\}})}^{\mathbf{D}_n^{\{S\}}} & \overbrace{\sum_{i=0}^{n} (\mathbf{S}_i^{\{S\}^{\mathsf{T}}} \mathbf{H}_i^{\mathsf{T}} \boldsymbol{\varUpsilon}_i^{-1} \mathbf{H}_i \mathbf{S}_i^{\{S^c\}})}^{\mathbf{D}_n^{\{S,S^c\}}} \\ \underbrace{\sum_{i=0}^{n} (\mathbf{S}_i^{\{S^c\}^{\mathsf{T}}} \mathbf{H}_i^{\mathsf{T}} \boldsymbol{\varUpsilon}_i^{-1} \mathbf{H}_i \mathbf{S}_i^{\{S\}})}_{\mathbf{D}_n^{\{S^c,S\}}} & \underbrace{\sum_{i=0}^{n} (\mathbf{S}_i^{\{S^c\}^{\mathsf{T}}} \mathbf{H}_i^{\mathsf{T}} \boldsymbol{\varUpsilon}_i^{-1} \mathbf{H}_i \mathbf{S}_i^{\{S^c\}})}_{\mathbf{D}_n^{\{S^c\}}} \end{bmatrix} \right)^{-1} = \begin{bmatrix} \mathbf{I}_s + \mathbf{D}_n^{\{S\}} & \mathbf{D}_n^{\{S,S^c\}} \\ \mathbf{D}_n^{\{S^c,S\}} & \mathbf{I}_{p-s} + \mathbf{D}_n^{\{S^c\}} \end{bmatrix}^{-1}, \tag{8.4}$$

where s is the cardinality of S, and $\mathbf{S}^{\{S\}} \in \mathbf{R}^{d \times s}$ and $\mathbf{S}^{\{S^c\}} \in \mathbf{R}^{d \times (p-s)}$ are the sensitivity matrices for $\boldsymbol{\theta}^{\{S\}}$ and $\boldsymbol{\theta}^{\{S^c\}}$, respectively, i.e. $\mathbf{S}^{\{S\}} = \nabla_{\boldsymbol{\theta}^{\{S\}}} \mathbf{x}$ and $\mathbf{S}^{\{S^c\}} = \nabla_{\boldsymbol{\theta}^{\{S^c\}}} \mathbf{x}$. Given the above decomposition, the marginal covariance of $\boldsymbol{\theta}^{\{S\}}$ given the measurements can be written as the Schur complement of the matrix $[\mathbf{I}_{p-s} + \sum_{i=0}^{n} (\mathbf{S}_i^{\{S^c\}^{\mathsf{T}}} \mathbf{H}_i^{\mathsf{T}} \boldsymbol{\varUpsilon}_i^{-1} \mathbf{H}_i \mathbf{S}_i^{\{S^c\}})]$ in $\mathcal{C}_n$ as follows:

$$\mathcal{C}_n^{\{S\}} = [(\mathbf{I}_s + \mathbf{D}_n^{\{S\}}) - (\mathbf{D}_n^{\{S,S^c\}})(\mathbf{I}_{p-s} + \mathbf{D}_n^{\{S^c\}})^{-1}(\mathbf{D}_n^{\{S^c,S\}})]^{-1} \tag{8.5}$$

and the information gain $\mathcal{I}_n^{\{S\}}$ as

$$\begin{aligned} \mathcal{I}_n^{\{S\}} &= -\frac{1}{2} \ln \left[\det (\mathcal{C}_n^{\{S\}}) \right] \\ &= \frac{1}{2} \ln \left[(\mathbf{I}_s + \mathbf{D}_n^{\{S\}}) - (\mathbf{D}_n^{\{S,S^c\}}) \right. \\ &\quad \left. (\mathbf{I}_{p-s} + \mathbf{D}_n^{\{S^c\}})^{-1} (\mathbf{D}_n^{\{S^c,S\}}) \right]. \end{aligned} \tag{8.6}$$

Another quantity of interest is the correlation between two subsets of parameters $\boldsymbol{\theta}^{\{S\}}$ and $\boldsymbol{\theta}^{\{W\}}$. In an information-theoretic context this can be assessed by how much more information is gained about the parameters $\boldsymbol{\theta}^{\{S\}}$ in addition to $\mathcal{I}_n^{\{S\}}$ if $\boldsymbol{\theta}^{\{W\}}$ was also known, i.e. the mutual information between $\boldsymbol{\theta}^{\{S\}}$ and $\boldsymbol{\theta}^{\{W\}}$ given the measurements. Similar to the procedure employed in equation (8.4), by splitting $\mathcal{C}_n$ into three components for $\boldsymbol{\theta}^{\{S\}}$, $\boldsymbol{\theta}^{\{W\}}$ and $\boldsymbol{\theta}^{\{(S \cup W)^c\}}$, one can write the conditional covariance $\mathcal{C}_n^{\{S|W\}}$ of the parameters $\boldsymbol{\theta}^{\{S\}}$ given the measurements and, additionally, the parameters $\boldsymbol{\theta}^{\{W\}}$ as follows:

$$\begin{aligned} \mathcal{C}_n^{\{S|W\}} = [(\mathbf{I}_s + \mathbf{D}_n^{\{S\}}) - (\mathbf{D}_n^{\{S,(S \cup W)^c\}})(\mathbf{I}_{p-s-w} \\ + \mathbf{D}_n^{\{(S \cup W)^c\}})^{-1}(\mathbf{D}_n^{\{(S \cup W)^c,S\}})]^{-1}, \end{aligned} \tag{8.7}$$

where w is the cardinality of W,

$$\mathbf{D}_n^{\{(S \cup W)^c\}} = \sum_{i=0}^{n} \left(\mathbf{S}_i^{\{(S \cup W)^c\}^{\mathsf{T}}} \mathbf{H}_i^{\mathsf{T}} \boldsymbol{\varUpsilon}_i^{-1} \mathbf{H}_i \mathbf{S}_i^{\{(S \cup W)^c\}} \right)$$

$$\text{with } \mathbf{S}^{\{(S \cup W)^c\}} = \nabla_{\boldsymbol{\theta}^{\{(S \cup W)^c\}}} \mathbf{x} \tag{8.8}$$

and

$$\mathbf{D}_n^{\{S,(S \cup W)^c\}} = \sum_{i=0}^{n} (\mathbf{S}_i^{\{S\}^{\mathsf{T}}} \mathbf{H}_i^{\mathsf{T}} \boldsymbol{\varUpsilon}_i^{-1} \mathbf{H}_i \mathbf{S}_i^{\{(S \cup W)^c\}}). \tag{8.9}$$

The information gain $\mathcal{I}_n^{\{S|W\}}$ about the parameters $\boldsymbol{\theta}^{\{S\}}$ given both the measurements and the parameters $\boldsymbol{\theta}^{\{W\}}$ is

$$\begin{aligned} \mathcal{I}_n^{\{S|W\}} &= -\frac{1}{2} \ln \left[\det (\mathcal{C}_n^{\{S|W\}}) \right] \\ &= \frac{1}{2} \ln \left[(\mathbf{I}_s + \mathbf{D}_n^{\{S\}}) - (\mathbf{D}_n^{\{S,(S \cup W)^c\}}) \right. \\ &\quad \left. \times (\mathbf{I}_{p-s-w} + \mathbf{D}_n^{\{(S \cup W)^c\}})^{-1} (\mathbf{D}_n^{\{(S \cup W)^c,S\}}) \right]. \end{aligned} \tag{8.10}$$

Lastly, the conditional mutual information (CMI), i.e. the additional (after the measurements are known) information gained about the parameters $\boldsymbol{\theta}^{\{S\}}$ due to the knowledge of $\boldsymbol{\theta}^{\{W\}}$ is

$$\mathcal{I}_n^{\{S;W\}} = \mathcal{I}_n^{\{S|W\}} - \mathcal{I}_n^{\{S\}}. \tag{8.11}$$

Remark 8.1. $\mathcal{I}_n^{\{S\}}$ is the gain in information about the parameters $\boldsymbol{\theta}^{\{S\}}$ given the measurements and when nothing is known about the parameters $\boldsymbol{\theta}^{\{S^c\}}$.

Remark 8.2. $\mathcal{I}_n^{\{S|W\}}$ is the gain in information about the parameters $\boldsymbol{\theta}^{\{S\}}$ given the measurements and the parameters $\boldsymbol{\theta}^{\{W\}}$, when nothing is known about the parameters $\boldsymbol{\theta}^{\{(S \cup W)^c\}}$.

Remark 8.3. In [21], the authors suggested a method to interpret the information gains $\mathcal{I}_n^{\{S\}}$ and $\mathcal{I}_n^{\{S|W\}}$ when the set S contained a single parameter by proposing a hypothetical measurement device. This is not necessary in the current formulation as all the distributions are approximated to be Gaussian. Therefore, when S contains only a single parameter, the conditional covariances $\mathcal{C}_n^{\{S\}}$ and $\mathcal{C}_n^{\{S|W\}}$ are scalar quantities representing the posterior variances of the parameter $\boldsymbol{\theta}^{\{S\}}$. When S contains more than one parameter, the quantities $\mathcal{I}_n^{\{S\}}$ and $\mathcal{I}_n^{\{S|W\}}$ are scalars that quantify the gains in information.
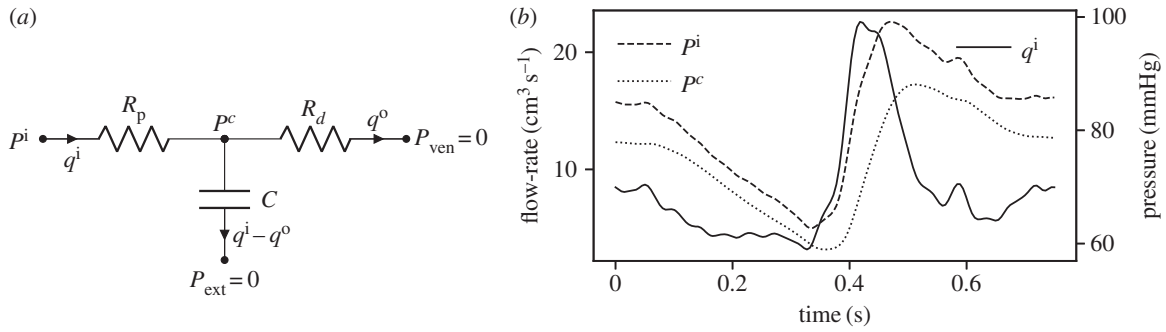
Figure 1. The three-element Windkessel model, flow-rate curve used, and pressure solutions. (a) Schematic of a three-element Windkessel model and (b) inlet flow-rate curve and Windkessel pressure solution, see equation (9.1), with nominal parameter values.

The above developed functions for information gains (and associated variances) are collectively referred as 'ISFs'. From this point onwards, the terms *marginal posterior variance* or just *marginal variance* for a parameter subset $\theta^{[S]}$ refers to the the variance conditioned on only the measurements, equation (8.5), and the corresponding information gain, equation (8.6), is referred as the *marginal information gain*. Similarly, the term *conditional variance* is used to refer to the variance when the measurements and additionally a parameter subset $\theta^{[W]}$ is given, equation (8.7), and the corresponding information gain is referred as the *conditional information gain*, equation (8.10). Lastly, the information shared between two subsets of parameters given the measurements, equation (8.11), is referred as the *conditional mutual information* or just the *mutual information*. Finally, the vector $\mathbf{z}_n = [\mathbf{y}_n^T, \mathbf{y}_{n-1}^T, \ldots, \mathbf{y}_0^T]^T$ is used to denote a collection of all measurement vectors up to time t_n.

9. Results and discussion

In this section, the theory developed above is applied to study three dynamical systems.

9.1. Three-element Windkessel model

Windkessel models are widely used to describe arterial haemodynamics [24]. Increasingly, they are also being used as boundary conditions in three-dimensional computational fluid dynamics simulations to assess patient-specific behaviour [20,25]. To perform patient-specific analysis, it is imperative that the parameters of the Windkessel model are estimated from measurements taken in each patient individually. A three-element Windkessel model is shown in figure 1a and consists of three parameters: R_{p} (proximal resistance) which represents the hydraulic resistance of large vessels; C (capacitance) which represents the compliance of large vessels; and R_d which represents the resistance of small vessels in the microcirculation. Note that these models use the electric analogy to fluid flow where pressure P is seen as voltage and flow-rate q is seen as electric current. Typically, inlet flow-rate q^{i} is measured (via magnetic resonance imaging or Doppler ultrasound) and inlet pressure P^{i} is measured by pressure catheters. The goal then is to estimate the parameters (R_{p}, C and R_d) by assuming q_i is deterministically known and minimizing the difference between the P^{i} reproduced by the model and the P_i that was measured. The model dynamics is described by the following differential

algebraic equations, which may also be rewritten as a single ODE:

$$
\left.
\begin{aligned}
\dot{P}^c &= \dot{P}_{\mathrm{ext}} + \frac{1}{C}(q^{\mathrm{i}} - q^{\mathrm{o}}), \\
P^c &= P_{\mathrm{ven}} + q^{\mathrm{o}} R_d \\
\text{and} \quad P^{\mathrm{i}} &= P^c + q^{\mathrm{i}} R_{\mathrm{p}},
\end{aligned}
\right\} \quad \text{with } P^{\mathrm{i}}(t=0) = P^{\mathrm{i}}_0, \quad (9.1)
$$

where P^{i} and P^c are the inlet and mid-Windkessel pressures, respectively, (figure 1a); P_{ext} and P_{ven} are the reference external and venous pressures, respectively, which are both set to zero; and q^{i} and q^{o} are the inlet and outlet flow-rates, respectively. The measurement model is written as follows:

$$
y_n = P^{\mathrm{i}}_n + \epsilon_n \quad \text{where } \epsilon_n \sim \mathcal{N}(0, \sigma^2_{\mathrm{noise}}), \quad (9.2)
$$

where ϵ_n is the noise (normally distributed with zero mean and variance $\sigma^2_{\mathrm{noise}}$) in measuring P^{i}_n to give the measurement y_n at time t_n. The measurement vector, therefore, has only one component $\mathbf{y}_n = [y_n]$. The nominal values of R_{p}, C, R_d are 0.838 mmHg·s cm^{-3}, 0.0424 cm^3 mmHg^{-1} and 9.109 mmHg·s cm^{-3}. Note that these units are chosen so that the results are comprehensible in typical units used in the clinic: millilitres for volume and millimetres of mercury for pressure. Figure 1b shows the inlet flow-rate q^{i} (taken from [20,26] where it was measured in the carotid artery of a healthy 27-year-old subject), and the resulting pressure curves obtained by the solution of equation (9.1) with $P^{\mathrm{i}}_0 = 85$ mmHg and nominal parameter values. To put a zero-mean and unit-variance prior on the parameters, see equation (4.8), the following parameter transformation is considered

$$
\xi = \xi_0 + \varsigma_\xi \theta_\xi \quad \text{where } \xi \in \{R_{\mathrm{p}}, C, R_d\}, \quad (9.3)
$$

where ξ represents the real parameter, ξ_0 and ς_ξ are transformation parameters, respectively, and θ_ξ represents the transformed parameter on which *a prior* of zero mean and unit variance is considered. Therefore, the prior considered on the real parameter ξ has mean ξ_0 and variance ς^2_ξ. The posterior variances for the transformed parameter θ_ξ and the real parameter ξ are represented by σ^2_θ and σ^2, respectively. A total of 150 time-points, evenly distributed between $t = 0$ s and $t = T_c$ (where $T_c = 0.75$s is the time period of the cardiac cycle), are used for the computation of ISFs and conditional variances.

Figure 2 shows the marginal posterior variances (conditional only on the measurements, (a–c)) and the corresponding information gains (d–f) for individual parameters at four different levels of measurement noises. The conditional variances when all measurements are taken into account, i.e. at $t = T_c$, are also summarized in table 1. An immediate utility of figure 2 is in identify intervals of time
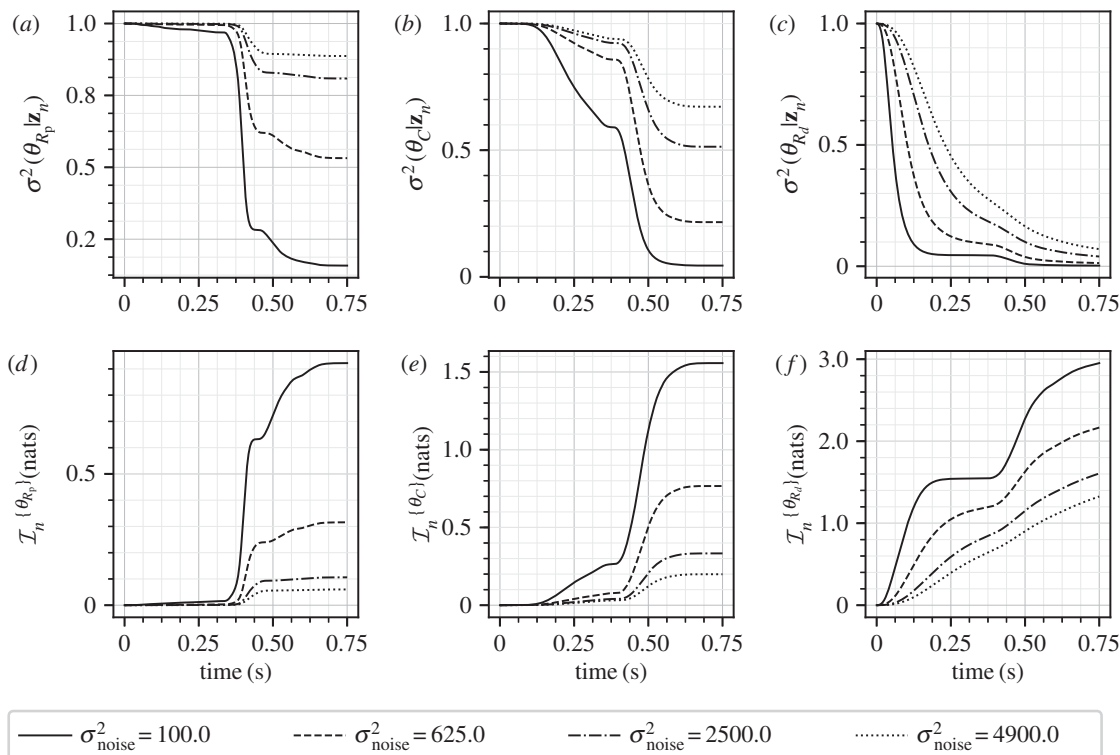
Figure 2. Marginal posterior variances $(a-c)$ and marginal information gains $(d-f)$ for the three Windkessel model parameters at four different levels of measurement noise.

where information is concentrated about a parameter. For example, from the first column it is clear that most of the information about the parameter θ_{R_p} is concentrated in the interval $t \in [0.3, 0.4]$ as this is the interval that shows maximum reduction in the marginal variance and highest information gain. This interval corresponds to the rising peak of the inlet flow-rate curve, see figure 1b, and from equation (9.1) it is clear that the parameter θ_{R_p} should have most effect on the pressure P^i in this interval. For the parameter θ_C, it appears from figure 2 that while information is available in the entire cardiac cycle, larger amount of information is concentrated in the later half of the cardiac cycle, $t \in [0.4, 0.75]$. For R_d information is available throughout the cardiac cycle. These observations have also been presented in [20] through the computation of GSFs [27] and in [21] through a Monte Carlo type computation of information gain. However, as opposed to GSFs which can be non-monotonic and therefore hard to interpret, the ISFs are always monotonic. Furthermore, since the GSFs are normalized by design, they are forced to start at 0 and end at 1, thereby making the assessment of measurement noise difficult. On the other hand, the effect of measurement noise is inherently built in to the ISFs. Figure 2 quantifies how increasing measurement noise results in a decreasing amount of information gained about the parameters. While this behaviour is intuitively expected, its quantification with respect to each individual parameter is made possible with the proposed method. For example, while at $\sigma^2_{\mathrm{noise}} = 100.0\,\mathrm{mmHg}^2$ the conditional variance of the parameter θ_{R_p} after considering all the measurements is 0.158 square units, at $\sigma^2_{\mathrm{noise}} = 4900.0\,\mathrm{mmHg}^2$ this conditional variance is 0.887 square units. Comparing this to the prior variance of 1.0 square units, one may conclude that at measurement noise of $4900.0\,\mathrm{mmHg}^2$ (standard deviation of 70.0 mmHg), the parameter R_p is extremely difficult to identify relative to

when the measurement noise is $100.0\,\mathrm{mmHg}^2$ (standard deviation of 10.0 mmHg). A similar argument can be made for the parameter θ_C, even though its identifiability is better than that of θ_{R_p} (θ_C has posterior variance of 0.672 square units at measurement noise of $\sigma^2_{\mathrm{noise}} = 4900.0\,\mathrm{mmHg}^2$). However, the parameter θ_{R_d} appears to be well identifiable even at $\sigma^2_{\mathrm{noise}} = 4900.0\,\mathrm{mmHg}^2$ with final posterior variance of 0.07 square units. This behaviour can be explained by the fact that measurement noise is assumed to be independent and identically distributed with zero mean at all measurement times. Therefore, the mean pressure is measured much more precisely than individual pressure measurements, irrespective of the noise levels, as when mean/expectation of equation (9.2) is taken, the expectation of noise component is zero:

$$\mathbb{E}[y_n] = \mathbb{E}[P^\mathrm{i}_n] + \mathbb{E}[\epsilon_n] = \mathbb{E}[P^\mathrm{i}_n], \qquad (9.4)$$

where $\mathbb{E}$ denotes the expectation operator. From equation (9.1) and figure 1a, the inlet mean pressure is equal to the inlet mean flow-rate times the sum of both resistances, i.e. $\mathbb{E}[P^\mathrm{i}_n] = (R_\mathrm{p} + R_d)\mathbb{E}[q^\mathrm{i}]$. Approximating $\mathbb{E}[y_n]$ by the sample mean as $(1/n)\sum_0^n y_i$, one obtains

$$\frac{1}{n}\sum_{i=0}^{n} y_i = (R_\mathrm{p} + R_d)\mathbb{E}[q^\mathrm{i}]. \qquad (9.5)$$

As q^i is assumed deterministic, from the above equation it can be seen that $R_\mathrm{p} + R_d$ is indirectly measured with high precision. As R_d is approximately an order of magnitude larger than R_p, it is natural that R_d dominates the sum $(R_\mathrm{p} + R_d)$ and hence, irrespective of the noise levels, a large amount of information is obtained about R_d (figure 2c,f). The order of magnitudes of the resistances are chosen by the physics of circulation, where the resistance of small vessels and microcirculation is significantly higher than that of large vessels [20,26], and is reflected in the chosen priors for the problem.

Table 1. Prior and posterior variances (marginal and conditional) for the Windkessel model.

	prior				expected posterior		
	θ-space		real space (ξ)		θ-space	real space (ξ)	
	mean	variance	mean	variance	variance	variance	std./prior-mean
parameter	μ_θ	σ_θ^2	$\mu = \xi_0$	$\sigma^2 = s_\xi^2$	σ_θ^2	σ^2	σ/ξ_0
observation noise, $\sigma_{noise}^2 = 100.0$							
R_p	0	1.0	8.40×10^{-1}	1.60×10^{-1}	1.58×10^{-1}	2.53×10^{-2}	18.9%
$R_p\|C$					1.41×10^{-1}	2.25×10^{-2}	17.9%
$R_p\|R_d$					8.13×10^{-2}	1.30×10^{-2}	13.6%
C	0	1.0	4.00×10^{-2}	4.00×10^{-4}	4.45×10^{-2}	1.78×10^{-5}	10.5%
$C\|R_p$					3.95×10^{-2}	1.58×10^{-5}	9.9%
$C\|R_d$					4.36×10^{-2}	1.74×10^{-5}	10.4%
R_d	0	1.0	9.11	2.03×10^{1}	2.73×10^{-3}	5.52×10^{-2}	2.6%
$R_d\|R_p$					1.40×10^{-3}	2.84×10^{-2}	1.8%
$R_d\|C$					2.67×10^{-3}	5.41×10^{-2}	2.6%
observation noise, $\sigma_{noise}^2 = 625.0$							
R_p	0	1.0	8.40×10^{-1}	0	5.32×10^{-1}	8.51×10^{-2}	34.7%
$R_p\|C$					5.04×10^{-1}	8.06×10^{-2}	33.8%
$R_p\|R_d$					3.51×10^{-1}	5.61×10^{-2}	28.2%
C	0	1.0	4.00×10^{-2}	0	2.16×10^{-1}	8.64×10^{-5}	23.2%
$C\|R_p$					2.04×10^{-1}	8.18×10^{-5}	22.6%
$C\|R_d$					2.16×10^{-1}	8.63×10^{-5}	23.2%
R_d	0	1.0	9.11	0	1.31×10^{-2}	2.66×10^{-1}	5.7%
$R_d\|R_p$					8.66×10^{-3}	1.75×10^{-1}	4.6%
$R_d\|C$					1.31×10^{-2}	2.65×10^{-1}	5.7%
observation noise, $\sigma_{noise}^2 = 2500.0$							
R_p	0	1.0	8.40×10^{-1}	0	8.09×10^{-1}	1.29×10^{-1}	42.8%
$R_p\|C$					7.98×10^{-1}	1.28×10^{-1}	42.5%
$R_p\|R_d$					6.75×10^{-1}	1.08×10^{-1}	39.1%
C	0	1.0	4.00×10^{-2}	0	5.14×10^{-1}	2.05×10^{-4}	35.8%
$C\|R_p$					5.07×10^{-1}	2.03×10^{-4}	35.6%
$C\|R_d$					5.13×10^{-1}	2.05×10^{-4}	35.8%
R_d	0	1.0	9.11	0	4.02×10^{-2}	8.15×10^{-1}	9.9%
$R_d\|R_p$					3.36×10^{-2}	46.80×10^{-1}	9.0%
$R_d\|C$					4.02×10^{-2}	8.13×10^{-1}	9.9%
observation noise, $\sigma_{noise}^2 = 4900.0$							
R_p	0	1.0	8.40×10^{-1}	0	8.87×10^{-1}	1.42×10^{-1}	44.8%
$R_p\|C$					8.82×10^{-1}	1.41×10^{-1}	44.7%
$R_p\|R_d$					7.99×10^{-1}	1.28×10^{-1}	42.6%
C	0	1.0	4.00×10^{-2}	0	6.72×10^{-1}	2.69×10^{-4}	41.0%
$C\|R_p$					6.68×10^{-1}	2.67×10^{-4}	40.9%
$C\|R_d$					6.70×10^{-1}	2.68×10^{-4}	40.9%
R_d	0	1.0	9.11	0	7.05×10^{-2}	1.43	13.1%
$R_d\|R_p$					6.35×10^{-2}	1.29	12.5%
$R_d\|C$					7.03×10^{-2}	1.42	13.1%
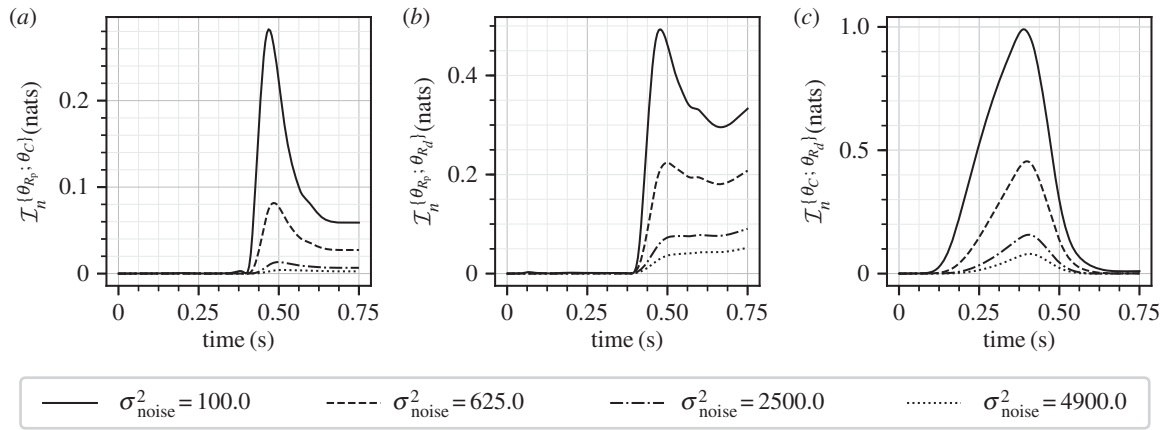
Figure 3. Mutual information between all the pairs of Windkessel model parameters at four different levels of measurement noise.
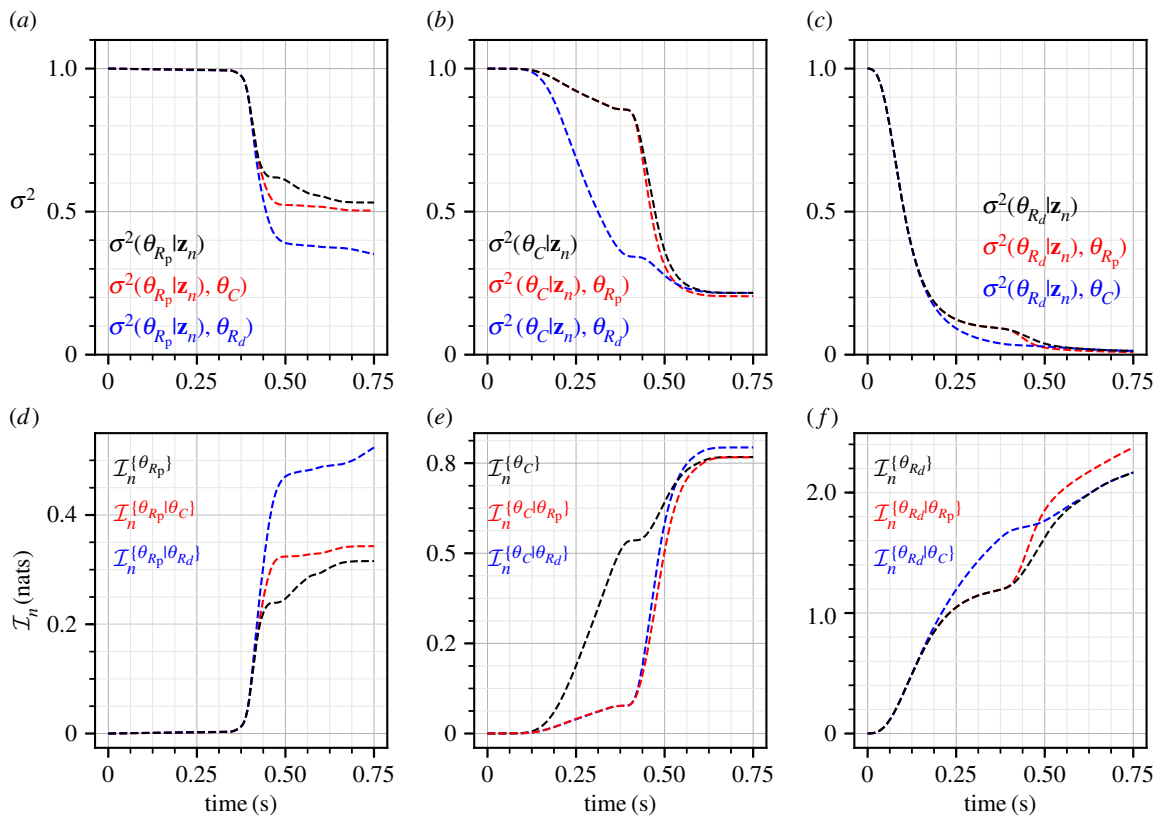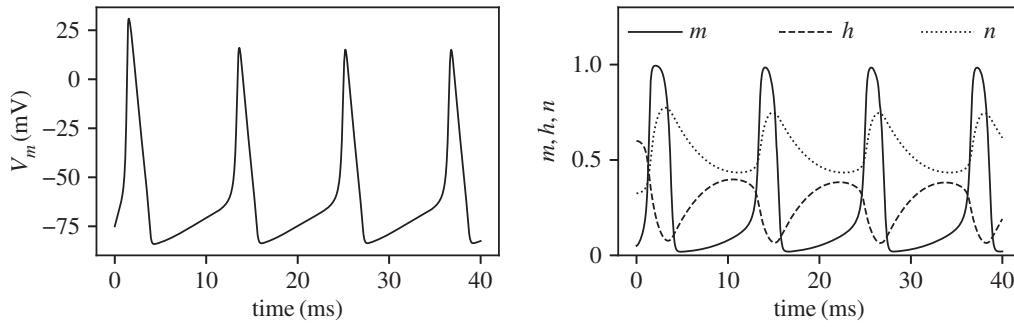

Figure 4. Conditional variances $(a-c)$ and conditional information gains $(d-f)$ for all pairs of the Windkessel model parameters. The measurement noise is $\sigma^2_{noise} = 625.0$.

Equation (9.5) and the arguments presented above imply that a significant amount of correlation must have been built up between the parameters R_p and R_d in the posterior distribution as the sum $(R_p + R_d)$ is measured with high precision. This correlation implies that if one of the parameters R_p or R_p were known then how much additional information can be gained about the other parameter. The CMI presented in equation (8.11) precisely measures this additional information. CMIs for all the three pairs of the parameters are shown in figure 3. It is clear that at the end of the cardiac cycle, the largest CMI is for the parameter pair θ_{R_p} and θ_{R_d}. It is sensible to compare the magnitude of CMIs with the marginal information gains (figure 2). For example, for the case of $\sigma^2_{noise} = 100.0$, the marginal gain in information about the parameter R_p is approximately 0.9 nats and the mutual

information between R_p and R_d is 0.35 nats; therefore, one may conclude that approximately 40% extra information about the parameter R_p is locked up in the correlation with R_d. For the pair R_d and C, it appears that correlation is built up in the $t \in [0.0, 0.4]$, the diastole, and destroyed in the remaining part, the systole, of the cardiac cycle. This can be explained by the fact that the time-constant $e^{-t/\tau}$, with $\tau = R_d C$, is the dominant parameter that governs the diastole phase [21] leading to a built up of correlation, and as independent information about C and R_d is acquired in systole (figure 2) this correlation is destroyed. It should be noted that these aspects, even without knowing the physics (or solution) of the problem, can be naturally inferred from figures 2 and 3.

The effect of correlations can be further assessed by looking at the conditional variances $(a-c)$ and conditional information

Figure 5. Solution of the Hodgkin–Huxley model, equation (9.6), for nominal parameter values.

gains (d–f) as depicted in figure 4. For $\sigma_{\text{noise}}^2 = 625.0$, this figure shows the conditional posterior variances and the conditional information gains for individual parameters when other parameters are given. For the parameter θ_{R_p}, it can be seen that the conditional variance given θ_{R_d} is lower than the marginal variance in the interval $t \in [0.4, 0.75]$ as this is the region where mutual information (correlation) is built between these parameters (figure 3). Similarly, in diastole, $t \in [0.0, 0.4]$, it can be seen that the conditional variance of parameter θ_C given θ_{R_d} is significantly lower as correlation is built up, but this gain quickly diminishes to zero in systole, $t \in [0.4, 0.75]$. For the parameter R_d, as a large amount of individual information is obtained marginally, the conditional variances are not too different than the marginal variances. Note, that the variances show an opposite behaviour to information gains as a decrease in variance implies gain in information. Therefore, even though the two measures appear to be similar, information gain is a better measure as it can be readily applied to cases where behaviour of a set of parameters is required to be studied. For example, if one was interested in the joint information again for a set of two parameters given a third, the information gain measure will be a scalar but the joint covariance will be a matrix. Furthermore, the relation between conditional information gain, marginal information gain, and mutual information is additive, see equation (8.11), whereas the relation between conditional variance and marginal variance is, in general, not additive. As a demonstration, it can be observed that the conditional information gain curves in figure 4 can be obtained by the addition of the corresponding curves from figures 2 and 3.

9.2. The Hodgkin–Huxley model of a neuron

The Hodgkin–Huxley model [28] describes ionic exchanges and their relationship to the membrane voltage in a biological neuron. This model has also been used as the basis for several other ionic models to describe a variety of excitable tissues such as cardiac cells [29]. The model is described by the following ODE equations:

$$\left.\begin{aligned} \dot{V}_{\text{m}} &= \frac{1}{C_{\text{m}}}\left[I_{\text{ext}} - \overbrace{g_{\text{Na}}m^3 h(V_{\text{m}} - V_{\text{Na}})}^{I_{\text{Na}}} - \overbrace{g_{\text{K}}n^4(V_{\text{m}} - V_{\text{K}})}^{I_{\text{K}}} \right.\\ &\qquad \left. - \underbrace{g_{\text{L}}(V_{\text{m}} - V_{\text{L}})}_{I_{\text{L}}} \right],\\ \dot{m} &= \alpha_m(V_{\text{m}})(1 - m) - \beta_m(V_{\text{m}})m,\\ \dot{h} &= \alpha_h(V_{\text{m}})(1 - m) - \beta_h(V_{\text{m}})h\\ \text{and}\quad \dot{n} &= \alpha_n(V_{\text{m}})(1 - m) - \beta_n(V_{\text{m}})n \end{aligned}\right\} \tag{9.6}$$

with

$$\left.\begin{aligned} \alpha_m(V_{\text{m}}) &= \frac{-0.1(V_{\text{m}} + 50)}{\exp\left(-(V_{\text{m}} + 50)/10\right) - 1},\\ \beta_m(V_{\text{m}}) &= 4\exp\left(\frac{-(V_{\text{m}} + 75)}{18}\right),\\ \alpha_h(V_{\text{m}}) &= 0.07\exp\left(\frac{-(V_{\text{m}} + 75)}{20}\right),\\ \beta_h(V_{\text{m}}) &= \frac{1.0}{\exp\left(-(V_{\text{m}} + 45)/10\right) + 1},\\ \alpha_n(V_{\text{m}}) &= \frac{-0.01(V_{\text{m}} + 65)}{\exp\left(-(V_{\text{m}} + 65)/10\right) - 1}\\ \text{and}\quad \beta_n(V_{\text{m}}) &= 0.125\exp\left(\frac{-(V_{\text{m}} + 75)}{80}\right), \end{aligned}\right\} \tag{9.7}$$

where V_{m} is the membrane voltage, C_{m} is the membrane capacitance, I_{ext} is the external current applied; I_{Na}, I_{K} and I_{L} are the sodium, potassium and leakage currents, respectively; V_{Na}, V_{K} and V_{L} are the equilibrium potentials for sodium, potassium and leakage ions, respectively; g_{Na}, g_{K} and g_{L} are the maximum conductances for the channels of sodium, potassium and leakage ions, respectively; and m, h and n are the dimensionless gate variables, $m, h, n \in [0, 1]$, that characterize the activation and inactivation of sodium and potassium channels. C_{m} is set to $1\,\mu\text{F cm}^{-2}$, and the equilibrium potentials are defined in millivolts (mV) relative to the membrane resting potential, E_{R}, as follows [30,31]:

$$\left.\begin{aligned} E_{\text{R}} &= -75\,\text{mV},\\ V_{\text{Na}} &= E_{\text{R}} + 115\,\text{mV},\\ V_{\text{K}} &= E_{\text{R}} - 12\,\text{mV}\\ \text{and}\quad V_{\text{L}} &= E_{\text{R}} + 10.613\,\text{mV}. \end{aligned}\right\} \tag{9.8}$$

The inverse problem is of estimating the three parameters g_{Na}, g_{K} and g_{L} by measuring the membrane voltage V_{m} when a constant external current $I_{\text{ext}} = 20\,\mu\text{A cm}^{-2}$ is applied to the neuron. It is well known that when a relatively high constant external current is applied the neuron exhibits a tonic spiking pattern in membrane voltage V_{m} [32–34]. With nominal parameter values of $g_{\text{Na}} = 120.0\,\text{mS cm}^{-2}$, $g_{\text{K}} = 36.0\,\text{mS cm}^{-2}$ and $g_{\text{L}} = 0.3\,\text{mS cm}^{-2}$, and initial conditions of $V_{\text{m}}(0) = -75$ mV, $m(0) = 0.05$, $h(0) = 0.6$ and $n(0) = 0.325$, this tonic spiking behaviour, generated by solving equation (9.6), is shown in figure 5. The observation model reads

$$y_n = V_{\text{m}_n} + \epsilon_n \quad \text{where } \epsilon_n \sim \mathcal{N}(0, \sigma_{\text{noise}}^2), \tag{9.9}$$

where V_{m_n} is the membrane voltage at time t_n and ϵ_n is the zero-mean measurement noise with variance σ_{noise}^2. As only V_{m} is measured the observation vector is $\mathbf{y}_n = [y_n]$. As opposed to the Windkessel case where the effect of noise is evaluated, in
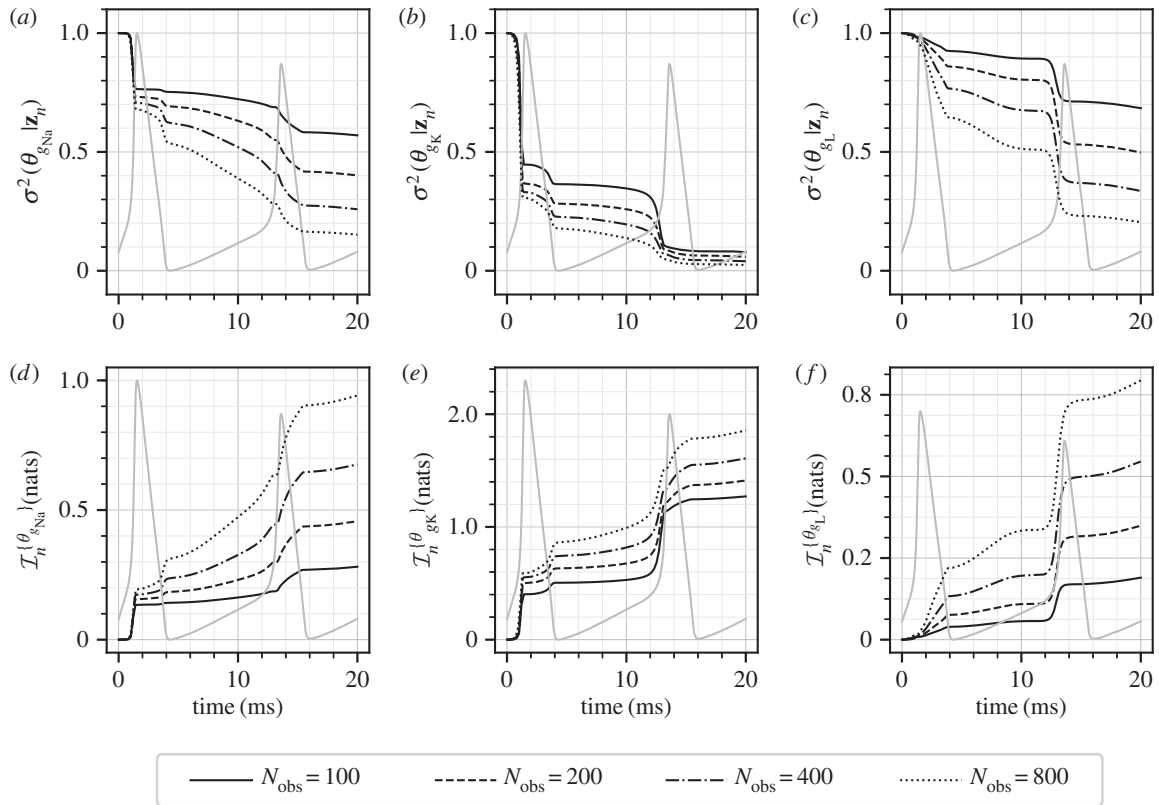
Figure 6. Marginal posterior variances $(a–c)$ and marginal information gains $(d–f)$ for all the Hodgkin–Huxley model parameters. Four different measurement frequencies are considered. In all the plots, an arbitrarily scaled V_m curve is shown in grey.
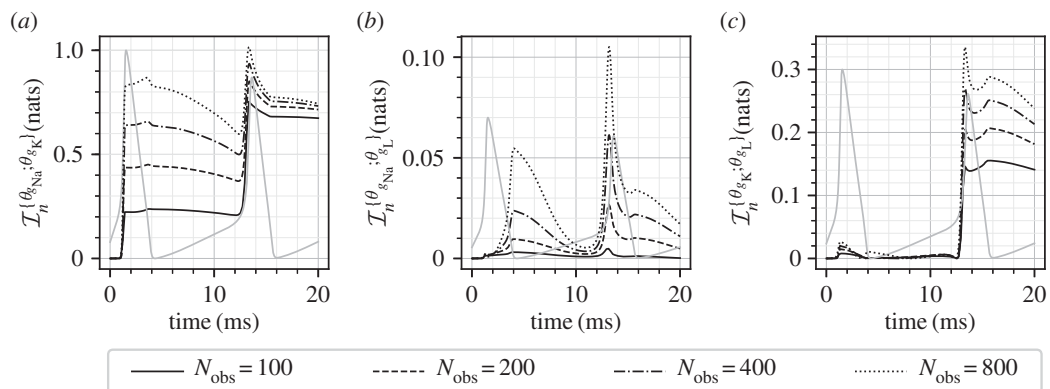

Figure 7. $(a–c)$ Mutual information between all the pairs of the parameters of the Hodgkin–Huxley model. Four different measurement frequencies are considered. In all the plots, an arbitrarily scaled V_m curve is shown in grey.

this case the effect of number of observations, i.e. the observation frequency is evaluated. N_{obs} number of measurement time-points evenly distributed in the time interval $t \in [0.0, 40.0]$ ms are studied. Four levels of observation frequencies resulting in four values of $N_{obs} \in \{100, 200, 400, 800\}$ are used while σ^2_{noise} is set to 100.0 mV^2 (standard deviation of 10.0 mV). Similar to the Windkessel example the following parametrization is used to impose zero-mean and unit-variance priors on the parameters.

$$\xi = \xi_0 + s_\xi \theta_\xi \quad \text{where } \xi \in \{g_{Na}, g_K, g_L\}, \qquad (9.10)$$

where ξ_0 is the nominal parameter value, zero-mean and unit-variance normal distribution prior is imposed on the transformed parameter θ_ξ, resulting in the prior distribution imposed on the real parameter ξ to be a normal distribution

with mean ξ_0 and variance s_ξ^2. The parameters s_ξ are set to 10.0, 6.0 and 0.1 mS cm^{-2} for g_{Na}, g_K and g_L, respectively.

Figure 6 shows the posterior marginal variances $(a–c)$ and the marginal information gains $(d–f)$ for the three parameters for all the four observation frequencies. In all these plots, an arbitrarily scaled $V_m(t)$ curve is shown in light grey for ease of interpretation relative to $V_m(t)$ variations. As expected, increasing the measurement frequency results in larger amounts of information (and consequently larger reduction in the posterior variances). However, it is observed that the parameters $\theta_{g_{Na}}$ and θ_{g_L} benefit most from an increase in measurement frequency as opposed to the parameter θ_{g_K} which benefits only marginally. This implies that at low observation frequencies the identifiability of θ_{g_K} is good, while very low amount of information is available for the parameters $\theta_{g_{Na}}$
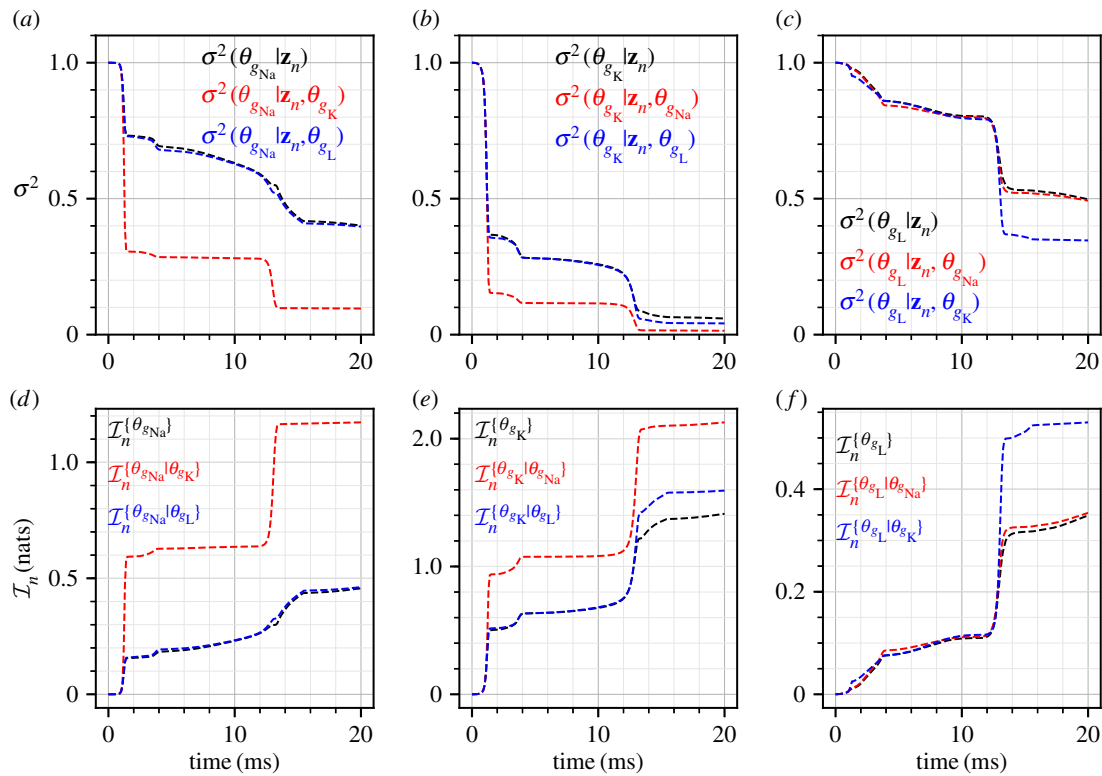
Figure 8. Conditional variances $(a-c)$ and conditional information gains $(d-f)$ for all pairs of the Hodgkin–Huxley model parameters. The case with $N_{obs} = 200$ is shown.

and θ_{g_L}. The behaviour for the parameter θ_{g_K} (figure 6b,e) shows that the information about this parameter is concentrated mostly in the sharp rising phase of the action potential V_m. A similar behaviour, although less salient, is observed for the parameters $\theta_{g_{Na}}$ and θ_{g_L} (figure 6a,d,c,f). While the Hodgkin–Huxley model is quite complex with gating variables of different time-constants and dependence of ionic currents on powers (up to fourth power) of the gating variables, it is widely understood that the rising phases of the action potential V_m are related to the sodium and potassium currents. This may explain why information about the parameters $\theta_{g_{Na}}$ and θ_{g_K} is mostly concentrated in this region. Furthermore, if we accept that the sodium and potassium currents, in combination, are responsible for the rising action potential, then we should also expect a substantial amount of correlation between the parameters $\theta_{g_{Na}}$ and θ_{g_K} as it should be hard to distinguish between these two parameters. This is precisely what is observed by the CMI analysis, figure 7, where a large amount of mutual information is developed between these two parameters. For the case of $N_{obs} = 100$, the marginal information gain in the parameter $\theta_{g_{Na}}$, figure 6, is approximately 0.3 nats, and it is observed from figure 7 that approximately 0.7 nats of mutual information exists between $\theta_{g_{Na}}$ and θ_{g_K}. This implies that the amount of information that can be gained about $\theta_{g_{Na}}$ by knowing θ_{g_K}, in addition to the measurements, is larger than the amount of information gained by just the measurements. Indeed, as the observation frequency is increased more information is available about all the parameters individually. Figure 7 also shows that significant amount of correlation is built between the parameters θ_{g_K} and θ_{g_L} during the sharp rising part of V_m. For example, for $N_{obs} = 200$, the amount of CMI between θ_{g_K} and θ_{g_L} is approximately 0.14 nats (figure 7), approximately the same magnitude as the marginal information gain of 0.15 nats (figure 6) for the

parameter θ_{g_L}. At the same time, since the marginal information gain for θ_{g_K} is approximately 1.25 nats (figure 6), the effect of this correlation, amounting to an information gain of 0.14 nats (figure 7), is not too significant for estimating θ_{g_K}.

Finally, the effect of the CMI, i.e. the correlation, can also be seen in terms of the conditional variances and conditional information gains as shown in figure 8 for $N_{obs} = 200$. As discussed above the correlations between the pairs $(\theta_{g_{Na}}, \theta_{g_K})$ and $(\theta_{g_K}, \theta_{g_L})$ show that the conditional variances are significantly lower (and the conditional information gain is larger) for one parameter when the other parameter is additionally known. It should be noted that the correlations and information gains presented are specific to the protocol, i.e. a constant external current resulting in tonic spiking of the neuron and only V_m being measured. The information gains will behave differently if the protocol is changed, for example to intermittent step currents or continuously varying external currents. Therefore, one application of the methods proposed in this article can be in optimal design of experiments, where one may design the protocol such that maximal information gain occurs for individual parameters while CMI (correlations in the posterior distribution) are minimized.
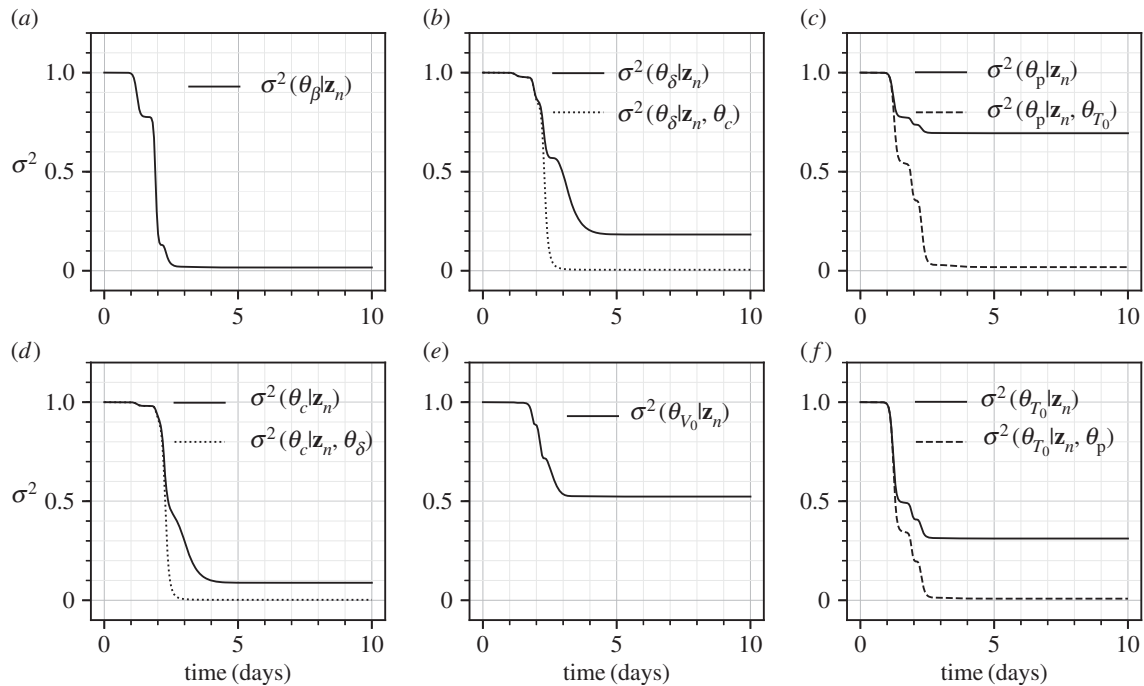
9.3. Influenza A virus kinetics

The final example presented is for the kinetics of the influenza A virus. The following model was proposed by Baccam *et al.* [35] to describe viral infection

$$
\left.
\begin{aligned}
\dot{V} &= pI - cV, \\
\dot{T} &= -\beta TV \\
\dot{I} &= \beta TV - \delta I,
\end{aligned}
\right\} \quad (9.11)
$$

and
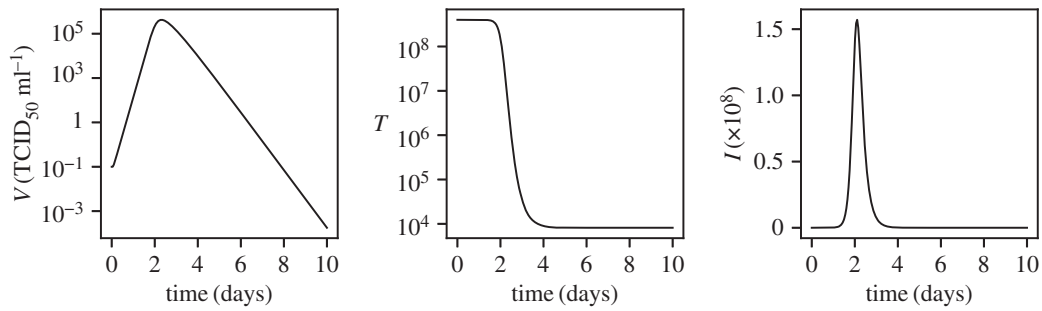
Figure 9. Solution of the influenza A kinetics model, equation (9.11), for nominal parameter values.

Figure 10. Marginal posterior variances (solid lines) and conditional variances (dashed lines) for the parameters of the influenza A kinetics model. Only V is measured with a measurement noise of $\sigma_{noise}^2 = 2.5 \times 10^7$ $(TCID_{50}\ ml^{-1})^2$.

where V is the infectious virus titre (measured in $TCID_{50}$ ml^{-1} of nasal wash), T is the number of uninfected target cells, I is the number of productively infected cells and $\{\beta, \delta, p, c\}$ are the model parameters. The parameter p represents the average rate at which the productively infected cells, I, increase the viral titres, and the parameter δ represents the rate at which the infected cells die. The parameter β characterises the rate at which the susceptible cells become infected and c represents the clearing rate of the virus.

As opposed to the previous example where the initial conditions were assumed to be known, in this example, the initial conditions for the virus titre V_0 and the number of uninfected target cells T_0 are considered unknown and hence form the parameters of the dynamical system. Time is measured in days (d) and the initial condition for the number of infected cells I_0 is assumed to be known at 0.0. Hence there are six parameters $[\beta, \delta, p, c, V_0, T_0]$ in total. The nominal values of the parameters are chosen to be $\beta = 2.7 \times 10^{-5}$ $(TCID_{50}\ ml^{-1})^{-1}$ d^{-1}, $\delta = 4.0$ d^{-1}, $p = 0.012$ $TCID_{50}\ ml^{-1} \cdot d^{-1}$, $c = 3.0$ d^{-1}, $V_0 = 0.1$ $TCID_{50}\ ml^{-1}$ and $T_0 = 4 \times 10^8$ based on the average patient parameters identified by Baccam et al. [35]. As in the previous examples, the following parametrization is

used to impose zero-mean and unit-variance priors on the transformed parameters:

$$\xi = \xi_0 + \varsigma_\xi \theta_\xi, \quad \text{where } \xi \in \{\beta, \delta, p, c, V_0, T_0\}, \qquad (9.12)$$

where θ_ξ represents the transformed version of the real parameter ξ, ξ_0 represents the nominal values of the parameter, and hence with a zero-mean and unit-variance prior on the transformed parameters θ_ξ, the prior imposed on the real parameter is of mean ξ_0 and variance ς_ξ^2. The scaling parameters ς_ξ are set to 9×10^{-06}, 1.3, 0.004, 1.0, 0.03 and 2.0×10^8 for β, δ, p, c, V_0 and T_0, respectively, in their respective units. The solution to equation (9.11) for the nominal parameter values is shown in figure 9. It is observed that both the virus titre V and the number of infected cells I increase sharply until they peak at the 2–3 day mark. After this a decrease in both values is observed. The number of uninfected target cells T remains approximately constant until the 2 day mark after which a sharp decrease (approx. 4 orders of magnitude) is observed over the next 2 days leading to a plateau.

To study the sensitivity and information gain two cases are considered: first, when only V is measured; and second, when both V and I are measured. In the first case, the observation model reads:

$$y_n = V_n + \epsilon_n \quad \text{where } \epsilon_n \sim \mathcal{N}(0, \sigma_{noise}^2), \qquad (9.13)$$
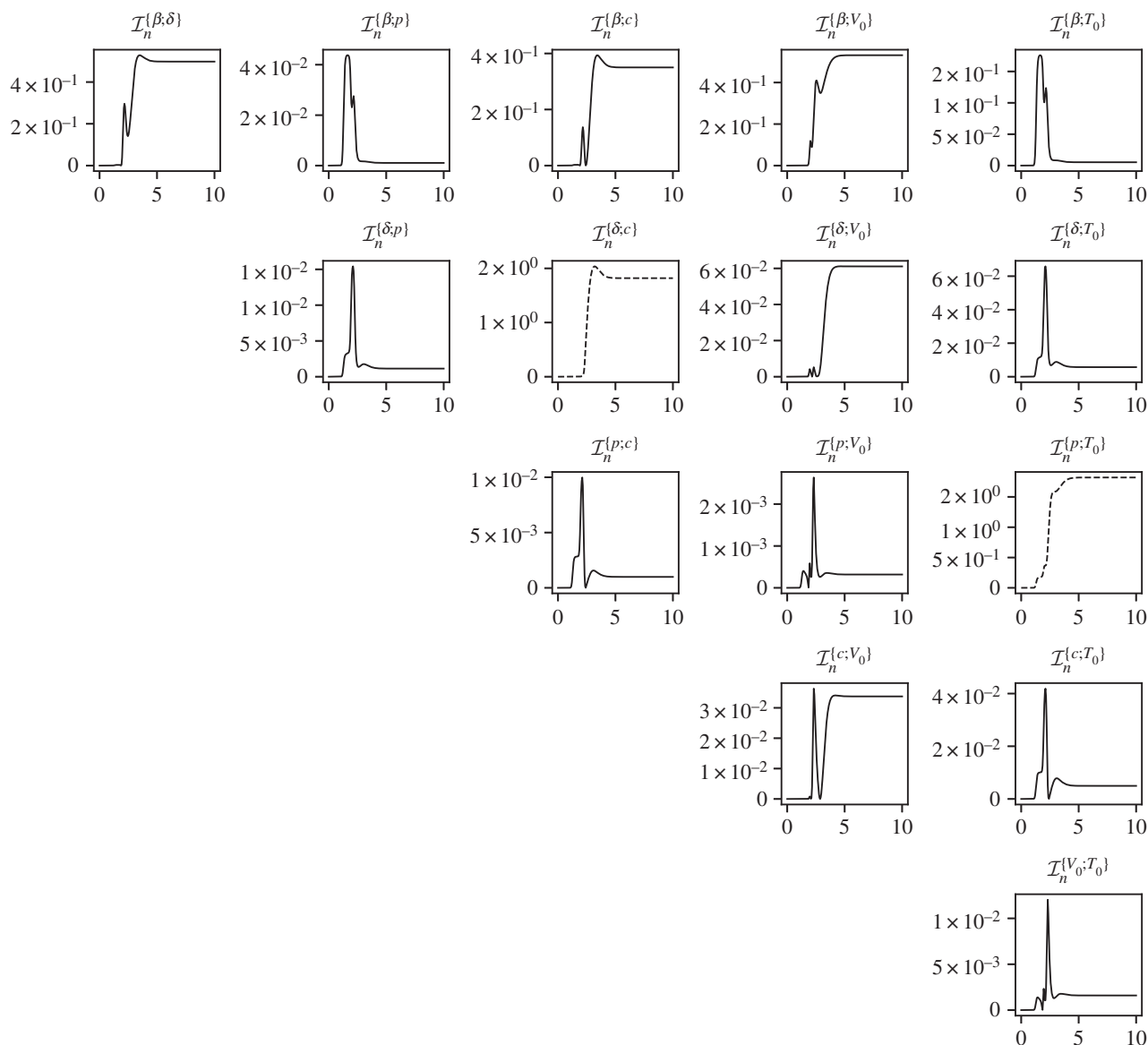
Figure 11. Mutual information between all pairs of the influenza A kinetics model. Pairs with significant (large) mutual information are plotted in dashed lines.

where V_n is the virus titre concentration at time t_n and ϵ_n is the zero-mean measurement noise with variance $\sigma_{noise}^2 = 2.5 \times 10^7$ $(TCID_{50} \, ml^{-1})^2$, i.e. a standard deviation of $5 \times 10^3 \, TCID_{50} \, ml^{-1}$. A total of 200 measurements are evenly distributed between 0 days and 10 days for the computation of marginal variances and information gains.

Figure 10 shows the marginal variances for all the parameters in solid lines and the conditional variances for a four pairs of parameters in dashed lines. Given the dynamics of the problem as shown in figure 9 it is not surprising that most of the information gain about all the parameters occurs in $t \in [0, 4]$ days. The parameters θ_β, θ_δ and θ_c appear to be well identifiable given the large decreases in marginal variances. However, the initial conditions θ_{V_0} and θ_{T_0} show less decrease in the variances indicating problems in their identifiability. Finally, the parameter p appears to be unidentifiable given that its marginal variance decreases from 1.0 (standard deviation 1.0) to only 0.7 square units (standard deviation 0.84 units). Figure 11 shows the mutual information between all the pairs of the parameters, where the parameter pairs that show a high mutual information are plotted in dashed lines. For the parameters in these

pairs of high mutual information, $(\theta_\delta, \theta_c)$ and (θ_p, θ_{T_0}), the conditional variances are plotted in figure 10. The parameter pair (θ_p, θ_{T_0}) is particularly interesting as the parameter θ_p, although unidentifiable individually, becomes very well identifiable, owing to the large mutual information it shares with T_0, if the initial condition T_0 is known. This observation was proved through classical methods by Miao et al. [6] where it was shown that taking higher-order derivatives of equation (9.11) and eliminating the unmeasured variables, T and I, one obtains the following differential equation:

$$\frac{d^3 V}{dt^3} = \left(\frac{d^2 V}{dt^2} + \delta c V + (\delta + c) \frac{dV}{dt} \right) \left(\frac{1}{V} \frac{dV}{dt} - \beta V \right)$$
$$- \delta c \frac{dV}{dt} - (\delta + c) \frac{d^2 V}{dt^2}. \tag{9.14}$$

As the above equation does not contain the parameter p, in the absence of any other quantity, i.e. T and I, and the corresponding initial conditions, the parameter p is not identifiable. Miao et al. [6] also reported that when T_0 is known, the parameter p becomes identifiable, which is consistent with the
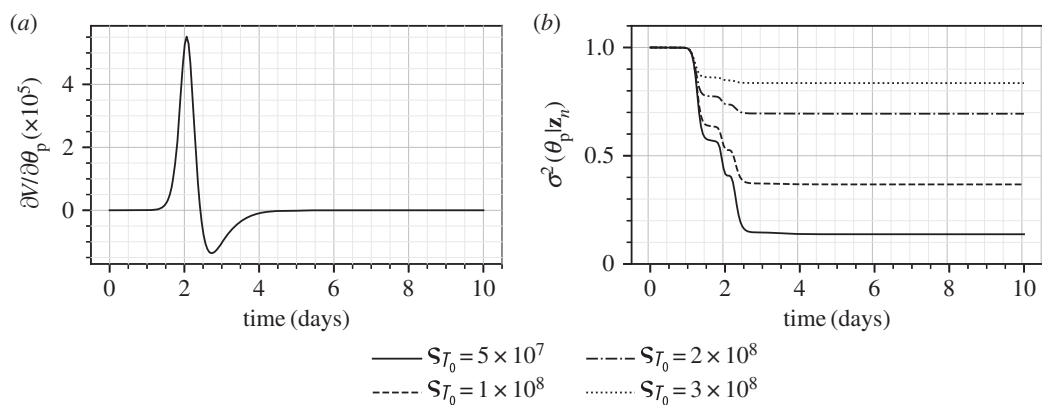
Figure 12. Sensitivity of the measurable V with respect to θ_p (a) and the marginal posterior variance of the parameter θ_p at different levels of s_{T_0} (b). The prior imposed on T_0 is of variance $s_{T_0}^2$.
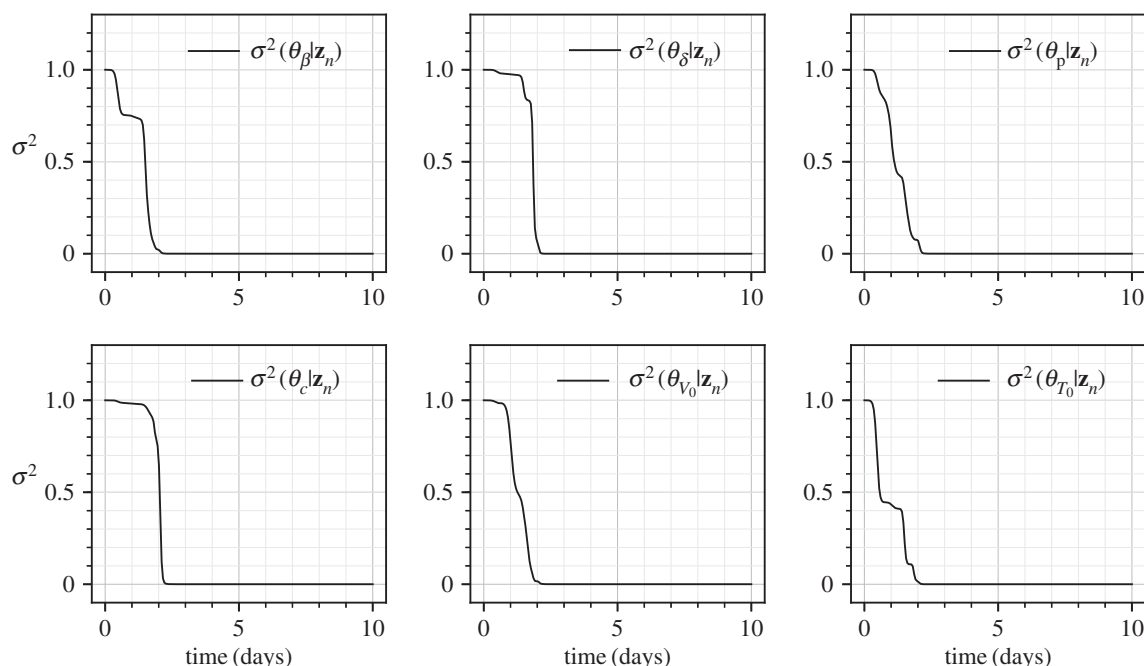
Figure 13. Marginal posterior variances for the parameters of the influenza A kinetics model. when both V and I are measured.

large mutual information. In the Bayesian approach adopted in this manuscript, a non-zero amount of knowledge (non-infinite variance) is inherently assumed in the prior for θ_{T_0}, which results in a small amount of information gain (and hence a small reduction in the marginal variance from 1.0 to 0.7 square units). This small amount of information gain is a result of the knowledge assumed in the prior. However, it is not significant enough to hide the identifiability problem for θ_P. One can choose to impose prior of higher ignorance by increasing the prior variance of the real parameter T_0 by increasing the scaling factor s_{T_0}. The results for four different values of s_{T_0} on the marginal variance of the parameter θ_p are shown in figure 12b. It is clear that a higher value of s_{T_0}, which implies higher ignorance in the prior for T_0, results in a decreasing amount of information gained about the parameter θ_p. This example shows how, without the use of classical analytical methods, see for example those presented in [6], which may not be easily applicable to all dynamical systems, the information theoretic approach can provide similar conclusions about parameter identifiability. Lastly, the classical sensitivity of the parameter p to the measurable V is shown in figure 12a,

whose large magnitude does not indicate any problems of parameter identifiability. Finally, Miao et al. [6] reported that all the parameters of the influenza dynamical system were well identifiable if both V and I, or both V and T were measured. For the case when both V and I are measured, the marginal variances are shown in figure 13, which too shows that no identifiability problems persist in this case. Note that the error structure in the measurement of I was assumed to be identical to the measurement of V, equation (9.13).

10. Conclusion

A new class of functions called the 'ISFs' have been proposed to study parametric information gain in a dynamical system. Based on a Bayesian and information-theoretic approach, such functions are easy to compute through classical sensitivity analysis. Compared to the previously proposed generalized sensitivity functions (GSFs) [27] to measure such information gain, the ISFs do not suffer from the forced-to-one behaviour and are easy to interpret as correlations are measured through

separate measures of mutual information as opposed to oscillations in GSFs. Furthermore, as opposed to GSFs, which are normalized, the ISFs can be used to compare information gain between different parameters and hence can be used to rank the parameters on ease of identifiability. They can be used to identify regions of high information content and indicate identifiability problems for parameters which show little to no information gain, or high mutual information (correlation) with other parameters. The application of ISFs is demonstrated on three models. For the Windkessel model, the effect of measurement noise is illustrated and it is shown that the insights provided by ISFs are consistent with those of a significantly more expensive Monte Carlo type approach [21]. For the Hodgkin–Huxley model, the effect of measurement frequency is illustrated, and finally, for the influenza A virus, it is shown how, even when classical sensitivity analysis fails to assess identifiability issues, the ISFs correctly reveal identifiability problems, which have been analytically proven through classical methods.

Appendix A. Differential analysis for equivalence of sensitivity and covariance evolution

From equation (3.2), the linearized dynamical system is

$$\dot{\mathbf{x}} = \mathbf{f}|_n + \nabla_{\mathbf{x}}\mathbf{f}|_n(\mathbf{x} - \boldsymbol{\mu}_{\mathbf{x}_n}) + \nabla_{\boldsymbol{\theta}}\mathbf{f}|_n(\boldsymbol{\theta} - \boldsymbol{\mu}_{\boldsymbol{\theta}}) + \nabla_t\mathbf{f}|_n(t - t_n). \tag{A1}$$

Separating the random variables $\boldsymbol{\theta}$ and $\mathbf{x}$ gives

$$\dot{\mathbf{x}} = \nabla_{\mathbf{x}}\mathbf{f}|_n\mathbf{x} + \nabla_{\boldsymbol{\theta}}\mathbf{f}|_n\boldsymbol{\theta}$$
$$+ \underbrace{(\mathbf{f}|_n - \nabla_{\mathbf{x}}\mathbf{f}|_n\boldsymbol{\mu}_{\mathbf{x}_n} - \nabla_{\boldsymbol{\theta}}\mathbf{f}|_n\boldsymbol{\mu}_{\boldsymbol{\theta}} + \nabla_t\mathbf{f}|_n(t - t_n))}_{\boldsymbol{\tau}_n}. \tag{A2}$$

Combined with trivial dynamics for the parameters $\dot{\boldsymbol{\theta}} = 0$, the dynamics for the combined vector $[\mathbf{x}^\mathsf{T}, \boldsymbol{\theta}^\mathsf{T}]^\mathsf{T}$ can be written as

$$\underbrace{\begin{bmatrix} \dot{\mathbf{x}} \\ \dot{\boldsymbol{\theta}} \end{bmatrix}}_{\dot{\boldsymbol{\varkappa}}} = \underbrace{\begin{bmatrix} \nabla_{\mathbf{x}}\mathbf{f}|_n & \nabla_{\boldsymbol{\theta}}\mathbf{f}|_n \\ \mathbf{O}_{p,d} & \mathbf{O}_{p,p} \end{bmatrix}}_{\mathcal{F}_n} \underbrace{\begin{bmatrix} \mathbf{x} \\ \boldsymbol{\theta} \end{bmatrix}}_{\boldsymbol{\varkappa}} + \underbrace{\begin{bmatrix} \boldsymbol{\tau}_n \\ \mathbf{O}_{p,1} \end{bmatrix}}_{\mathfrak{r}_n}, \tag{A3}$$

where $\mathbf{O}_{a,b}$ represents a zero matrix of size $a \times b$. The above is concisely written as

$$\dot{\boldsymbol{\varkappa}} = \mathcal{F}_n\boldsymbol{\varkappa} + \mathfrak{r}_n. \tag{A4}$$

For the above stochastic differential equation, it is well known, see for example [36], that the covariance matrix of $\boldsymbol{\varkappa}$, denoted by $\boldsymbol{\Xi}$, evolves according to the following differential equation:

$$\dot{\boldsymbol{\Xi}} = \mathcal{F}_n\boldsymbol{\Xi} + \boldsymbol{\Xi}\mathcal{F}_n^\mathsf{T}. \tag{A5}$$

Therefore, if the covariance matrix of $\boldsymbol{\varkappa}_n$ is

$$\boldsymbol{\Xi} = \mathbf{Cov}\left(\begin{bmatrix} \mathbf{x} \\ \boldsymbol{\theta} \end{bmatrix}\right) = \begin{bmatrix} \boldsymbol{\Sigma}_{n,n} & \boldsymbol{\Lambda}_{n,\boldsymbol{\theta}} \\ \boldsymbol{\Lambda}_{\boldsymbol{\theta},n}^\mathsf{T} & \boldsymbol{\Sigma}_{\boldsymbol{\theta},\boldsymbol{\theta}} \end{bmatrix}, \tag{A6}$$

then $\boldsymbol{\Xi}$ evolves according to equation (A5) as

$$\dot{\boldsymbol{\Xi}} = \begin{bmatrix} \nabla_{\mathbf{x}}\mathbf{f}|_n & \nabla_{\boldsymbol{\theta}}\mathbf{f}|_n \\ \mathbf{O}_{p,d} & \mathbf{O}_{p,p} \end{bmatrix}\begin{bmatrix} \boldsymbol{\Sigma}_{n,n} & \boldsymbol{\Lambda}_{n,\boldsymbol{\theta}} \\ \boldsymbol{\Lambda}_{\boldsymbol{\theta},n} & \boldsymbol{\Sigma}_{\boldsymbol{\theta},\boldsymbol{\theta}} \end{bmatrix} + \begin{bmatrix} \boldsymbol{\Sigma}_{n,n} & \boldsymbol{\Lambda}_{n,\boldsymbol{\theta}} \\ \boldsymbol{\Lambda}_{\boldsymbol{\theta},n} & \boldsymbol{\Sigma}_{\boldsymbol{\theta},\boldsymbol{\theta}} \end{bmatrix}\begin{bmatrix} \nabla_{\mathbf{x}}^\mathsf{T}\mathbf{f}|_n & \mathbf{O}_{d,p} \\ \nabla_{\boldsymbol{\theta}}^\mathsf{T}\mathbf{f}|_n & \mathbf{O}_{p,p} \end{bmatrix}$$
$$= \begin{bmatrix} \nabla_{\mathbf{x}}\mathbf{f}|_n\boldsymbol{\Sigma}_{n,n} + \nabla_{\boldsymbol{\theta}}\mathbf{f}|_n\boldsymbol{\Lambda}_{n,\boldsymbol{\theta}}^\mathsf{T} + \boldsymbol{\Sigma}_{n,n}\nabla_{\mathbf{x}}^\mathsf{T}\mathbf{f}|_n + \boldsymbol{\Lambda}_{n,\boldsymbol{\theta}}\nabla_{\boldsymbol{\theta}}^\mathsf{T}\mathbf{f}|_n & \nabla_{\mathbf{x}}\mathbf{f}|_n\boldsymbol{\Lambda}_{n,\boldsymbol{\theta}} + \nabla_{\boldsymbol{\theta}}\mathbf{f}|_n\boldsymbol{\Sigma}_{\boldsymbol{\theta},\boldsymbol{\theta}} \\ \boldsymbol{\Lambda}_{n,\boldsymbol{\theta}}^\mathsf{T}\nabla_{\mathbf{x}}^\mathsf{T}\mathbf{f}|_n + \boldsymbol{\Sigma}_{\boldsymbol{\theta},\boldsymbol{\theta}}\nabla_{\boldsymbol{\theta}}^\mathsf{T}\mathbf{f}|_n & \mathbf{O}_{p,p} \end{bmatrix}. \tag{A7}$$

The next task is to relate the above evolution of the covariance matrix with the evolution of sensitivity matrix. From equation (2.6), the sensitivity matrix $\mathbf{S}$ evolves as

$$\dot{\mathbf{S}} = \nabla_{\mathbf{x}}\mathbf{f}|_n\mathbf{S}_n + \nabla_{\boldsymbol{\theta}}\mathbf{f}|_n. \tag{A8}$$

Therefore, taking the transpose of equation (A8) yields

$$(\dot{\mathbf{S}})^\mathsf{T} = \left(\frac{\mathrm{d}\mathbf{S}}{\mathrm{d}t}\right)^\mathsf{T} = \frac{\mathrm{d}(\mathbf{S}^\mathsf{T})}{\mathrm{d}t} = \mathbf{S}_n^\mathsf{T}\nabla_{\mathbf{x}}^\mathsf{T}\mathbf{f}|_n + \nabla_{\boldsymbol{\theta}}^\mathsf{T}\mathbf{f}|_n. \tag{A9}$$

The derivative of the matrix product $\mathbf{S}\mathbf{S}^\mathsf{T}$ can be written as follows:

$$\frac{\mathrm{d}(\mathbf{S}\mathbf{S}^\mathsf{T})}{\mathrm{d}t} = \mathbf{S}\frac{\mathrm{d}(\mathbf{S}^\mathsf{T})}{\mathrm{d}t} + \frac{\mathrm{d}(\mathbf{S})}{\mathrm{d}t}\mathbf{S}^T. \tag{A10}$$

Substituting the derivatives from (A8) with (A9) into the above equation gives

$$\frac{\mathrm{d}(\mathbf{S}\mathbf{S}^\mathsf{T})}{\mathrm{d}t} = \mathbf{S}\mathbf{S}^\mathsf{T}\nabla_{\mathbf{x}}^\mathsf{T}\mathbf{f}|_n + \nabla_{\mathbf{x}}\mathbf{f}|_n\mathbf{S}\mathbf{S}^\mathsf{T} + \nabla_{\boldsymbol{\theta}}\mathbf{f}|_n\mathbf{S}^\mathsf{T} + \mathbf{S}\nabla_{\boldsymbol{\theta}}^\mathsf{T}\mathbf{f}|_n. \tag{A11}$$

It is easy to see that if $\boldsymbol{\Sigma}_{\boldsymbol{\theta},\boldsymbol{\theta}} = \mathbf{I}_p$, $\boldsymbol{\Lambda}_{n,\boldsymbol{\theta}} = \mathbf{S}$ and $\boldsymbol{\Sigma}_{n,n} = \mathbf{S}\mathbf{S}^\mathsf{T}$, then the state covariance, $\boldsymbol{\Sigma}_{n,n}$, and the cross-covariance, $\boldsymbol{\Lambda}_{n,\boldsymbol{\theta}}$, from equation (A7) evolve as

$$\dot{\boldsymbol{\Sigma}}_{n,n} = \mathbf{S}\mathbf{S}^\mathsf{T}\nabla_{\mathbf{x}}^\mathsf{T}\mathbf{f}|_n + \nabla_{\mathbf{x}}\mathbf{f}|_n\mathbf{S}\mathbf{S}^\mathsf{T} + \nabla_{\boldsymbol{\theta}}\mathbf{f}|_n\mathbf{S}^\mathsf{T} + \mathbf{S}\nabla_{\boldsymbol{\theta}}^\mathsf{T}\mathbf{f}|_n$$
$$= \frac{\mathrm{d}(\mathbf{S}\mathbf{S}^\mathsf{T})}{\mathrm{d}t} \tag{A12}$$

and

$$\dot{\boldsymbol{\Lambda}}_{n,\boldsymbol{\theta}} = \nabla_{\mathbf{x}}\mathbf{f}|_n\mathbf{S}_n + \nabla_{\boldsymbol{\theta}}\mathbf{f}|_n = \dot{\mathbf{S}}. \tag{A13}$$

Appendix B. Asymptotic analysis of the conditional covariance

In this section, the behaviour of the conditional covariance matrix $\mathcal{C}_n$ as $n \to \infty$ is considered. From equation (5.4), A_n

can be written as

$$\mathbf{A}_n = \mathbf{B}_n \mathbf{B}_n^\mathsf{T} + \boldsymbol{\Gamma}_n, \tag{B 1}$$

where $\boldsymbol{\Gamma}_n$ is a diagonal matrix with elements as follows:

$$\Gamma_{i,i} = \boldsymbol{Y}_i; \quad 0 \le i \le n. \tag{B 2}$$

By applying the Kailath variant of the Sherman–Morrison–Woodbury identity the inverse of $\mathbf{A}_n$ can be expanded as

$$\mathbf{A}_n^{-1} = \boldsymbol{\Gamma}_n^{-1} - \boldsymbol{\Gamma}_n^{-1}\mathbf{B}_n(\mathbf{I}_p + \mathbf{B}_n^\mathsf{T}\boldsymbol{\Gamma}_n^{-1}\mathbf{B}_n)^{-1}\mathbf{B}_n^\mathsf{T}\boldsymbol{\Gamma}_n^{-1}. \tag{B 3}$$

Plugging this in equation (6.3) yields

$$\mathcal{C}_n = \mathbf{I}_p - \mathbf{B}_n^\mathsf{T}\boldsymbol{\Gamma}_n^{-1}\mathbf{B}_n + \mathbf{B}_n^\mathsf{T}\boldsymbol{\Gamma}_n^{-1}\mathbf{B}_n(\mathbf{I}_p + \mathbf{B}_n^\mathsf{T}\boldsymbol{\Gamma}_n^{-1}\mathbf{B}_n)^{-1}\mathbf{B}_n^\mathsf{T}\boldsymbol{\Gamma}_n^{-1}\mathbf{B}_n \tag{B 4}$$

$$= \mathbf{I}_p - \mathbf{D}_n + \mathbf{D}_n(\mathbf{I}_p + \mathbf{D}_n)^{-1}\mathbf{D}_n, \tag{B 5}$$

where

$$\mathbf{D}_n = \mathbf{B}_n^\mathsf{T}\boldsymbol{\Gamma}_n^{-1}\mathbf{B}_n. \tag{B 6}$$

The matrix D is symmetric, and can be factorized by singular value decomposition (SVD) as follows

$$\mathbf{D}_n = \mathbf{U}_n \boldsymbol{\Phi}_n \mathbf{U}_n^\mathsf{T}, \tag{B 7}$$

with

$$\mathbf{U}_n \mathbf{U}_n^\mathsf{T} = \mathbf{I}_p \tag{B 8}$$

and $\boldsymbol{\Phi}_n$ is a diagonal matrix with diagonal entries equal to the eigenvalues, λ_i, of $\mathbf{D}_n$.

$$\boldsymbol{\Phi}_{n_{i,i}} = \lambda_i. \tag{B 9}$$

Owing to the symmetric nature of $\mathbf{D}_n$, all the eigenvalues are real. Furthermore, if $\mathbf{D}_n$ is positive-definite then all eigenvalues are positive. Substituting $\mathbf{D}_n$ from equation (B 6) in equation (B 4) yields

$$\mathcal{C}_n = \mathbf{I}_p - \mathbf{U}_n\boldsymbol{\Phi}_n\mathbf{U}_n^\mathsf{T} + \mathbf{U}_n\boldsymbol{\Phi}_n\mathbf{U}_n^\mathsf{T}(\mathbf{I}_p + \mathbf{U}_n\boldsymbol{\Phi}_n\mathbf{U}_n^\mathsf{T})^{-1}\mathbf{U}_n\boldsymbol{\Phi}_n\mathbf{U}_n^\mathsf{T} \tag{B 10}$$

$$= \mathbf{I}_p - \mathbf{U}_n\boldsymbol{\Phi}_n\mathbf{U}_n^\mathsf{T} + \mathbf{U}_n\boldsymbol{\Phi}_n\mathbf{U}_n^\mathsf{T}(\mathbf{U}_n\mathbf{U}_n^\mathsf{T} + \mathbf{U}_n\boldsymbol{\Phi}_n\mathbf{U}_n^\mathsf{T})^{-1}\mathbf{U}_n\boldsymbol{\Phi}_n\mathbf{U}_n^\mathsf{T} \tag{B 11}$$

$$= \mathbf{I}_p - \mathbf{U}_n\boldsymbol{\Phi}_n\mathbf{U}_n^\mathsf{T} + \mathbf{U}_n\boldsymbol{\Phi}_n\mathbf{U}_n^\mathsf{T}(\mathbf{U}_n(\mathbf{I}_p + \boldsymbol{\Phi}_n)\mathbf{U}_n^\mathsf{T})^{-1}\mathbf{U}_n\boldsymbol{\Phi}_n\mathbf{U}_n^\mathsf{T} \tag{B 12}$$

$$= \mathbf{U}_n\mathbf{U}_n^\mathsf{T} - \mathbf{U}_n\boldsymbol{\Phi}_n\mathbf{U}_n^\mathsf{T} + \mathbf{U}_n\boldsymbol{\Phi}_n(\mathbf{I}_p + \boldsymbol{\Phi}_n)^{-1}\boldsymbol{\Phi}_n\mathbf{U}_n^\mathsf{T} \tag{B 13}$$

$$= \mathbf{U}_n\underbrace{[\mathbf{I}_p - \boldsymbol{\Phi}_n + \boldsymbol{\Phi}_n(\mathbf{I}_p + \boldsymbol{\Phi}_n)^{-1}\boldsymbol{\Phi}_n]}_{\mathbf{P}_n}\mathbf{U}_n^\mathsf{T}. \tag{B 14}$$

In the above $\mathbf{P}_n$ is a diagonal matrix with the entries

$$P_{n_{i,i}} = 1 - \lambda_i + \frac{\lambda_i^2}{1 + \lambda_i} = \frac{1}{1 + \lambda_i}. \tag{B 15}$$

If the minimum eigenvalue of $\mathbf{D}_n$ is much larger than 1, i.e.

$$\min_i \lambda_i \gg 1, \tag{B 16}$$

then

$$P_{n_{i,i}} \approx \frac{1}{\lambda_i} \tag{B 17}$$

and

$$\mathbf{P}_n \approx \boldsymbol{\Phi}^{-1}. \tag{B 18}$$

Consequently, equation (B 10) yields

$$\mathcal{C}_n \approx \mathbf{U}_n\boldsymbol{\Phi}^{-1}\mathbf{U}_n^\mathsf{T} = \mathbf{D}_n^{-1}. \tag{B 19}$$

Finally, from the above and equations (B 5), (B 2) and (5.5), the conditional covariance matrix can be written as

$$\mathcal{C}_n \approx \left(\sum_{i=0}^{n}(\mathbf{S}_i^\mathsf{T}\mathbf{H}_i^\mathsf{T}\boldsymbol{Y}_i^{-1}\mathbf{H}_i\mathbf{S}_i)\right)^{-1}. \tag{B 20}$$

It can hence be concluded that if the minimum eigenvalue of $\mathbf{D}_n$ monotonically increases as n increases then

$$\lim_{n\to\infty}\mathcal{C}_n = \left(\sum_{i=0}^{n}(\mathbf{S}_i^\mathsf{T}\mathbf{H}_i^\mathsf{T}\boldsymbol{Y}_i^{-1}\mathbf{H}_i\mathbf{S}_i)\right)^{-1}. \tag{B 21}$$

Let the eigenvalues of $\mathbf{D}_n$ be denoted in decreasing order as $\lambda_1(\mathbf{D}_n) \ge \lambda_2(\mathbf{D}_n) \ge \ldots \ge \lambda_p(\mathbf{D}_n)$. The behaviour of the minimum eigenvalue of $\lambda_p(\mathbf{D}_n)$ is of concern. Note that $\mathbf{D}_n$ can be written as

$$\mathbf{D}_n = \sum_{i=0}^{n}(\mathbf{S}_i^\mathsf{T}\mathbf{H}_i^\mathsf{T}\boldsymbol{Y}_i^{-1}\mathbf{H}_i\mathbf{S}_i). \tag{B 22}$$

Consequently,

$$\mathbf{D}_{n+1} = \mathbf{D}_n + \underbrace{\mathbf{S}_{n+1}^\mathsf{T}\mathbf{H}_{n+1}^\mathsf{T}\boldsymbol{Y}_{n+1}^{-1}\mathbf{H}_{n+1}\mathbf{S}_{n+1}}_{\mathbf{Q}_{n+1}}. \tag{B 23}$$

$\mathbf{D}_n$ and $\mathbf{Q}_n$ are both symmetric matrices. Let the eigenvalues of $\mathbf{Q}_{n+1}$ be denoted in decreasing order as $\lambda_1(\mathbf{Q}_{n+1}) \ge \lambda_2(\mathbf{Q}_{n+1}) \ge \ldots \ge \lambda_p(\mathbf{Q}_{n+1})$. From equation (B 19) one has

$$\mathrm{Tr}(\mathbf{D}_{n+1}) = \mathrm{Tr}(\mathbf{D}_n) + \mathrm{Tr}(\mathbf{Q}_{n+1}), \tag{B 24}$$

where Tr denotes the trace. Expressed in terms of the eigenvalues of the respective matrices, the above reads

$$\sum_{i=1}^{p}\lambda_i(\mathbf{D}_{n+1}) = \sum_{i=1}^{p}\lambda_i(\mathbf{D}_n) + \sum_{i=1}^{p}\lambda_i(\mathbf{Q}_{n+1}). \tag{B 25}$$

From several inequalities on the sums of eigenvalues of Hermitian matrices, specifically the *Ky Fan inequality* [37,38], one has

$$\sum_{i=1}^{r}\lambda_i(\mathbf{D}_{n+1}) \le \sum_{i=1}^{r}\lambda_i(\mathbf{D}_n) + \sum_{i=1}^{r}\lambda_i(\mathbf{Q}_{n+1}); \quad r \le p. \tag{B 26}$$

Substituting $r = p - 1$ in equation (B 22) and subtracting it from equation (B 21) results in

$$\lambda_p(\mathbf{D}_{n+1}) \ge \lambda_p(\mathbf{D}_n) + \lambda_p(\mathbf{Q}_{n+1}). \tag{B 27}$$

Consequently, if $\mathbf{Q}_{n+1}$ is full rank then $\lambda_p(\mathbf{Q}_{n+1}) > 0$ and

$$\lambda_p(\mathbf{D}_{n+1}) > \lambda_p(\mathbf{D}_n), \tag{B 28}$$

which implies that the minimum eigenvalue of $\mathbf{D}_n$ is monotonically increasing.

The above results are put in the perspective of classical nonlinear regression analysis [9,10] by assuming that the observation operator $\mathbf{H}_i$ is equal to identity for all i. Then, under a further assumption that $\mathbf{Q}_i = (\nabla_{\boldsymbol{\theta}}^\mathsf{T}\mathbf{x}|_i)\boldsymbol{Y}_i^{-1}(\nabla_{\boldsymbol{\theta}}\mathbf{x}|_i)$ is full-rank for all i, the conditional covariance matrix of the parameter is

$$\lim_{n\to\infty}\mathcal{C}_n = \mathcal{M}^{-1}, \tag{B 29}$$

where $\mathcal{M}$ is the Fisher information matrix defined as

$$\mathcal{M} = \sum_{i=0}^{n}[(\nabla_{\boldsymbol{\theta}}^\mathsf{T}\mathbf{x}|_i)\boldsymbol{Y}_i^{-1}(\nabla_{\boldsymbol{\theta}}\mathbf{x}|_i)]. \tag{B 30}$$

Appendix C. Conditional covariance for finite n

From equation (B 10) one has

$$\mathcal{C}_n = \mathbf{U}_n \mathbf{P}_n \mathbf{U}_n^{\mathsf{T}}, \qquad (C\,1)$$

where P_n is given by equation (B 11). Consider the matrix $(\mathbf{D}_n + \mathbf{I}_p)^{-1}$, which can be expanded as

$$(\mathbf{D}_n + \mathbf{I}_p)^{-1} = (\mathbf{U}_n \boldsymbol{\Phi}_n \mathbf{U}_n^{\mathsf{T}} + \mathbf{I}_p)^{-1} \qquad (C\,2)$$

$$= (\mathbf{U}_n \boldsymbol{\Phi}_n \mathbf{U}_n^{\mathsf{T}} + \mathbf{U}_n \mathbf{U}_n^{\mathsf{T}})^{-1} \qquad (C\,3)$$

$$= (\mathbf{U}_n (\boldsymbol{\Phi}_n + \mathbf{I}_p) \mathbf{U}_n^{\mathsf{T}})^{-1} \qquad (C\,4)$$

$$= \mathbf{U}_n (\boldsymbol{\Phi}_n + \mathbf{I}_p)^{-1} \mathbf{U}_n^{\mathsf{T}} \qquad (C\,5)$$

$$= \mathbf{U}_n \mathbf{P}_n \mathbf{U}_n^{\mathsf{T}} = \mathcal{C}_n. \qquad (C\,6)$$

Following the above and equation (B 18), the conditional covariance matrix can be written as

$$\mathcal{C}_n = \left(\mathbf{I}_p + \sum_{i=0}^{n} (\mathbf{S}_i^{\mathsf{T}} \mathbf{H}_i^{\mathsf{T}} \mathbf{Y}_i^{-1} \mathbf{H}_i \mathbf{S}_i) \right)^{-1}. \qquad (C\,7)$$

References

1. Saltelli A, Chan K, Scott EM. 2000 *Sensitivity analysis*, vol. 1. New York, NY: Wiley.

2. Degenring D, Froemel C, Dikta G, Takors R. 2004 Sensitivity analysis for the reduction of complex metabolism models. *J. Process Control* **14**, 729–745. (doi:10.1016/j.jprocont.2003.12.008)

3. Jacquez JA. 1985 *Compartmental analysis in biology and medicine*, vol. 2. Ann Arbor, MI: University of Michigan Press.

4. Yao KZ, Shaw BM, Kou B, McAuley KB, Bacon D. 2003 Modeling ethylene/butene copolymerization with multi-site catalysts: parameter estimability and experimental design. *Polymer React. Eng.* **11**, 563–588. (doi:10.1081/PRE-120024426)

5. Quaiser T, Mönnigmann M. 2009 Systematic identifiability testing for unambiguous mechanistic modeling—application to JAK-STAT, MAP kinase, and NF-κB signaling pathway models. *BMC Syst. Biol.* **3**, 50. (doi:10.1186/1752-0509-3-50)

6. Miao H, Xia X, Perelson AS, Wu H. 2011 On identifiability of nonlinear ODE models and applications in viral dynamics. *SIAM Rev.* **53**, 3–39. (doi:10.1137/090757009)

7. Frieden BR. 2004 *Science from Fisher information: a unification*. Cambridge, UK: Cambridge University Press.

8. Rodriguez-Fernandez M, Egea JA, Banga JR. 2006 Novel metaheuristic for parameter estimation in nonlinear dynamic biological systems. *BMC Bioinformatics* **7**, 483. (doi:10.1186/1471-2105-7-483)

9. Seber GA, Wild C. 1989 *Nonlinear regression: Wiley series in probability and mathematical statistics*. Chichester, UK: Wiley.

10. Banks TH, Davidian M, Samuels Jr JR, Sutton KL. 2009 An inverse problem statistical methodology summary. In *Mathematical and statistical estimation approaches in epidemiology*, pp. 249–302. Berlin, Germany: Springer.

11. Ashyraliyev M, Blom J. 2008 On parameter estimation and determinability for the model of pattern formation in *Drosophila melanogaster*. In *Modelling, Analysis and Simulation -MAS 2008, 17–19 September, Calabria, Italy*. E0802

12. Raue A, Kreutz C, Maiwald T, Bachmann J, Schilling M, Klingmüller U, Timmer J. 2009 Structural and practical identifiability analysis of partially observed dynamical models by exploiting the profile likelihood. *Bioinformatics* **25**, 1923–1929. (doi:10.1093/bioinformatics/btp358)

13. Raue A, Becker V, Klingmüller U, Timmer J. 2010 Identifiability and observability analysis for experimental design in nonlinear dynamical models. *Chaos* **20**, 045105. (doi:10.1063/1.3528102)

14. Raue A, Kreutz C, Maiwald T, Klingmüller U, Timmer J. 2011 Addressing parameter identifiability by model-based experimentation. *IET Syst. Biol.* **5**, 120–130. (doi:10.1049/iet-syb.2010.0061)

15. Li P, Vu QD. 2013 Identification of parameter correlations for parameter estimation in dynamic biological models. *BMC Syst. Biol.* **7**, 91. (doi:10.1186/1752-0509-7-91)

16. Li P, Vu QD. 2015 A simple method for identifying parameter correlations in partially observed linear dynamic models. *BMC Syst. Biol.* **9**, 92. (doi:10.1186/s12918-015-0234-3)

17. Bai P et al. 2007 Stochastic and deterministic models for agricultural production networks. *Math Biosci. Eng.* **4**, 373–402. (doi:10.3934/mbe.2007.4.373)

18. Batzel J, Baselli G, Mukkamala R, Chon KH. 2009 Modelling and disentangling physiological mechanisms: linear and nonlinear identification techniques for analysis of cardiovascular regulation. *Phil. Trans. R. Soc. A* **367**, 1377–1391. (doi:10.1098/rsta.2008.0266)

19. Banks H, Dediu S, Ernstberger SL, Kappel F. 2010 Generalized sensitivities and optimal experimental design. *J. Inv. Ill-Posed Probl.* **18**, 25–83. (doi:10.1515/jiip.2010.002)

20. Pant S, Fabrèges B, Gerbeau JF, Vignon-Clementel IE. 2014 A methodological paradigm for patient-specific multi-scale CFD simulations: from clinical measurements to parameter estimates for individual analysis. *Int. J. Numer. Method Biomed. Eng.* **30**, 1614–1648. (doi:10.1002/cnm.2692)

21. Pant S, Lombardi D. 2015 An information-theoretic approach to assess practical identifiability of parametric dynamical systems. *Math. Biosci.* **268**, 66–79. (doi:10.1016/j.mbs.2015.08.005)

22. Van Trees HL. 2004 *Detection, estimation, and modulation theory*. New York, NY: John Wiley & Sons.

23. Bay S, Herzet C, Brossier JM, Barbot JP, Geller B. 2008 Analytic and asymptotic analysis of Bayesian Cramér–Rao bound for dynamical phase offset estimation. *IEEE Trans. Signal Process.* **56**, 61–70. (doi:10.1109/TSP.2007.906760)

24. Westerhof N, Lankhaar JW, Westerhof BE. 2009 The arterial Windkessel. *Med. Biol. Eng. Comput.* **47**, 131–141. (doi:10.1007/s11517-008-0359-2)

25. Vignon-Clementel IE, Alberto Figueroa C, Jansen KE, Taylor CA. 2006 Outflow boundary conditions for three-dimensional finite element modeling of blood flow and pressure in arteries. *Comput. Methods. Appl. Mech. Eng.* **195**, 3776–3796. (doi:10.1016/j.cma.2005.04.014)

26. Vignon-Clementel IE, Figueroa C, Jansen K, Taylor C. 2010 Outflow boundary conditions for 3D simulations of non-periodic blood flow and pressure fields in deformable arteries. *Comput. Methods Biomech. Biomed. Eng.* **13**, 625–640. (doi:10.1080/10255840903413565)

27. Thomaseth K, Cobelli C. 1999 Generalized sensitivity functions in physiological system identification. *Ann. Biomed. Eng.* **27**, 607–616. (doi:10.1114/1.207)

28. Hodgkin AL, Huxley AF. 1952 A quantitative description of membrane current and its application to conduction and excitation in nerve. *J. Physiol.* **117**, 500–544. (doi:10.1113/jphysiol.1952.sp004764)

29. Noble D. 1966 Applications of Hodgkin–Huxley equations to excitable tissues. *Physiol. Rev.* **46**, 1–50. (doi:10.1152/physrev.1966.46.1.1)

30. Lloyd CM, Lawson JR, Hunter PJ, Nielsen PF. 2008 The CellML model repository. *Bioinformatics* **24**, 2122–2123. (doi:10.1093/bioinformatics/btn390)

31. Hodgkin AL, Huxley AF. 1952 A quantitative description of membrane current and its application to conduction and excitation in nerve (Original Model+Stimulus). *CellML* See https://models.cellml.org/exposure/5d116522c3b43ccaeb87a1 ed10139016/hodgkin_huxley_1952.cellml/view (26 September 2017).

32. Izhikevich EM. 2004 Which model to use for cortical spiking neurons? *IEEE Trans. Neural Netw.* **15**, 1063–1070. (doi:10.1109/TNN.2004.832719)

33. Hasegawa H. 2000 Responses of a Hodgkin–Huxley neuron to various types of spike-train inputs. *Phys. Rev. E* **61**, 718. (doi:10.1103/PhysRevE.61.718)

34. Koch C. 2004 *Biophysics of computation: information processing in single neurons*. Oxford, UK: Oxford university press.

35. Baccam P, Beauchemin C, Macken CA, Hayden FG, Perelson AS. 2006 Kinetics of influenza A virus infection in humans. *J. Virol.* **80**, 7590–7599. (doi:10.1128/JVI.01623-05)

36. Gelb A. 1974 *Applied optimal estimation*. Cambridge, MA: MIT press.

37. Fulton W. 2000 Eigenvalues, invariant factors, highest weights, and Schubert calculus. *Bull. Am. Math. Soc.* **37**, 209–249. (doi:10.1090/S0273-0979-00-00865-X)

38. Fan K. 1949 On a theorem of Weyl concerning eigenvalues of linear transformations I. *Proc. Natl Acad. Sci. USA* **35**, 652–655. (doi:10.1073/pnas.35.11.652)

Correction

Correction to 'Information sensitivity functions to assess parameter information gain and identifiability of dynamical systems'

Sanjay Pant

SP, 0000-0002-2081-308X

The funding statement and reference [10] should be revised as follows:

Reference

10. Banks HT, Davidian M, Samuels Jr JR, Sutton KL. 2009 An inverse problem statistical methodology summary. In *Mathematical and statistical estimation approaches in epidemiology* (eds G Chowell, JM Hyman, LMA Bettencourt, C Castillo-Chavez), pp. 249–302. Dordrecht, The Netherlands: Springer.

THE ROYAL SOCIETY
PUBLISHING